Stability design for frame type structures

Delft University of Technology
Faculty of Civil Engineering and Geoscience
Section of Structural Mechanics

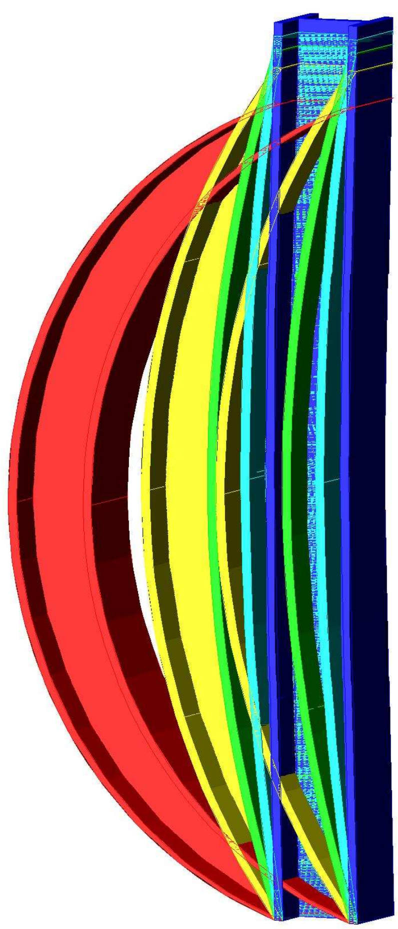

Master thesis report
Ing. R. P. Veerman

Stability design for frame type structures

Delft University of Technology
Faculty of Civil Engineering and Geoscience
Section of Structural Mechanics

Master thesis report

by

Ing. R. P. Veerman

Examination committee:
Prof. ir. A. C. W. M. Vrouwenvelder
Prof. Ir. F. S. K. Bijlaard
Dr. Ir. P. C. J. Hoogenboom
Ir. L. J. M. Houben

Preface

This document is the main report of the master thesis: Stability design for frame type structures. The study has been carried out at the section Structural Mechanics of Delft University of Technology, Department of Civil Engineering. This report contains description, calculation methods and results for several stability problems. The background, the analyses and the calculations can be found in an Appendix report.

I would like to thank those who made it possible to finish this thesis.

Special thanks to the members of the examination committee:
- Prof. ir. A. C. W. M. Vrouwenvelder
- Prof. ir. F. S. K. Bijlaard
- Dr. ir. P. C. J. Hoogenboom

Delft, July 2009
Ing. R. P. Veerman

Summary

It is well known that the buckling load of structures and structural members strongly depends on residual stresses and shape deviations. Traditionally, these imperfections are included in empirical formulas, which correct the buckling load that is computed without imperfections. The objective of the research presented in this thesis is to study whether structural models that are extended with realistic physical imperfections can predict structural capacities accurately. To this end four structural types have been analyzed: a single column, an unbraced portal frame, a braced portal frame and a braced extended frame.

Every structural type has been analysed analytically. The results are several formulas to calculate the additional deflection. Based on the total deflection, the internal stresses can be calculated. The internal stresses result in an ultimate load. The obtained formulas are different for each structural type and could not be generalized.

Each structural type has also been analysed numerically by introducing imperfections in a structural analysis program. This program (Matrix Frame) is often used in engineering practice. Residual stresses could not be added to the cross-section stresses because we had no access to the program source code. However, this was circumvented by including residual stresses as a reduced cross-section stiffness.

The results obtained by the analytical analysis, the numerical analysis and empirical code equations have been compared. In some situations significant differences occur. The reason can be modelling inaccuracies, analysis approximations or conservatism in code equations. It can be concluded that realistic physical imperfections can be used to replace empirical code equations. However, introducing this in everyday practice might be not easy. More research is needed in measuring imperfections, numerical analysis and calibrations to current codes of practice.

Index

Chapter 1 Introduction

The force flow in most structures can be accurately computed by linear elastic analyses. However, in some structures second order effects can be important, for example unbraced frames with a large vertical loading. For these structures second order analyses need to be performed. In current practice the computations are performed by software. The second order deformation under service loading is determined by an iterative algorithm. The member capacities and structural capacity under ultimate loading are checked by applying the governing code equations.

Note that there is a remarkable difference in the computation for service loading and for ultimate loading. The computation for service loading is based on “pure structural mechanics” and the computation for ultimate loading is based on “best practice”. The reason is that structural mechanics alone strongly overestimates the structural capacity because it neglects the influence of residual stresses and shape deviations. Organisations that developed the structural codes recognised the importance of these imperfections a long time ago. Therefore, the codes are based on extensive experimental programs designed to determine the true member capacities.

The objective of the research presented in this thesis is to study whether structural models that are extended with residual stresses and shape deviations can predict structural capacities accurately. In other words; can pure structural mechanics be extended with clear physical properties such that we no longer need to use black box code rules for determining structural capacities?

To this end four structural types have been analyzed:

- A single column, loaded by a centric compression force.
- An unbraced portal frame, loaded by a uniformly distributed load.
- A braced portal frame, loaded by a uniformly distributed load.
- A braced extended frame, loaded by a uniformly distributed load.

Each type has been analysed following an analytical approach. Full use was made of the modern features of mathematical software. Some types were also analysed by using a standard frame analysis program. To this end a trick was developed and tested for including the effects of residual stresses.

Chapter 2 Column

The buckling load of a simply supported column depends on the dimensions and the shape of the section. In addition, the buckling load strongly depends on shape imperfections and residual stresses. (Inhomogeneous steel quality is not taken into account in this study.)

2.1 Buckling of a perfect column

Consider a column pinned at both ends and loaded by a compressive normal force *N*. At a certain load (the Euler buckling load) there are two equilibrium situations possible. In the first equilibrium situation the column remains straight. In the second equilibrium situation the column deflects in a half sine shape. The amount of deflection is unknown. See Appendix A for the derivation. The Euler buckling load can be calculated by the following formula:

$$F_E = \frac{\pi^2 EI}{{L_{buc}}^2}$$

where

F_E = Euler buckling load

L_{buc} = Buckling length

EI = Bending stiffness

Suppose a column is loaded by a horizontal load and the deflection results in a half sine shape. If this column is also loaded by a compressive force, the deflection increases (second order effect). The following formula can be used to calculate the total deflection of the column.

$$u = e\frac{F_E}{F_E - N}$$

or

$$u = e\frac{n}{n-1} \quad \text{with } n = \frac{F_E}{N}$$

where

N = Compression force

F_E = Euler buckling load

e = Initial deflection

u = Total deflection (including initial deflection)

2.2 Imperfections

There are many ways to produce steel sections, for example welding, rolling and cold forming. This study is based on the HEA series. HEA sections are rolled. In the factory a block of steal is rolled en flattened. See Figures 2.1 and 2.2 for some illustrations. A perfectly flattening process is not possible. This results in shape imperfections.

The imperfections vary over the length of the section. In this study it is assumed that the shape imperfections can be described by a half sine function (Fig. 2.3). The maximum eccentricity is in the middle of the section. According to the Dutch code this maximum is one thousands of the column length (NEN 6771 art. 10.2.5).

If the weight of the column is not taken into account, the normal force is constant over the length. The bending moment is the multiplication of the normal force and the eccentricity. The bending moment is largest when the eccentricity is largest. Therefore, the most critical cross-section is the middle of a column. The bending moments result in additional compressive stress in the right flange and a reduction of the compressive stress in the left flange (Fig. 2.3).

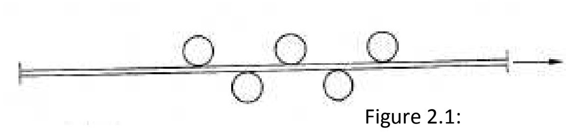

Figure 2.1:
Flattening

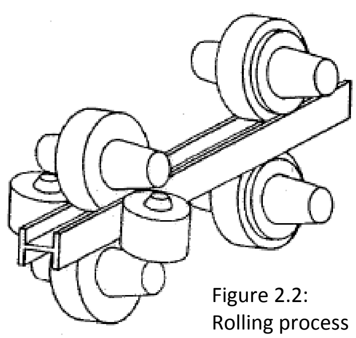

Figure 2.2:
Rolling process

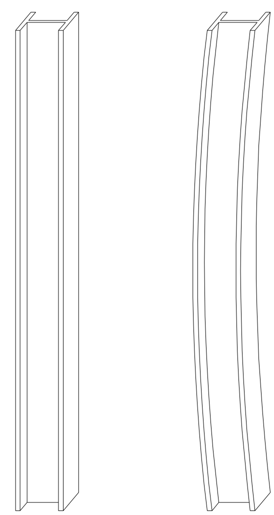

Figure 2.3:
Imperfections

2.3 Residual stress

Before starting the rolling process, the section is heated. Due to rolling the temperature is further increased. The cooling down speed is not constant in the section. The cooling down speed depends on the ratio volume/surface. At the tips of the flanges and in the middle of the web this ratio is small and the cooling down process is fast. At the intersection between the flanges and the web this ratio is large and cooling down process is slow. This results in compression stress in the tips of the flanges and tensile stress in the intersection points (Fig. 2.4). These stresses are called residual stresses, initial stresses or rolling stresses.

Residual stresses are always in equilibrium. Therefore, there are no residual section moments or residual section normal forces. The rolling stresses are always smaller than the yield stress. The production method and the cross-section dimensions influence the amount of residual stress.

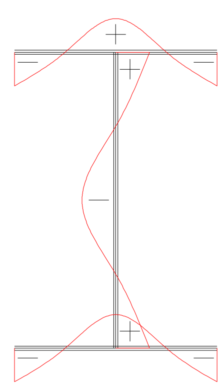

Figure 2.4:
Residual stress
distribution in a I
section

Consider a perfectly straight homogenous I section which has residual stresses. Suppose this section is loaded by a centric compressive force only. At increasing load, the combination of residual stress and compressive stress results in local yielding. The tips of the flanges and the middle of the web yield first. The section yields partially, but will not fail. The structure fails when the whole section yields. The presents of residual stress does not influence the yield load.

Consider a homogenous I section with residual stresses and a shape imperfection. When the column is loaded by a compressive force the deflection increases. The increase of the deflection depends on the moment of inertia. If the tips of the flanges yield, the effective moment of inertia decreases. This results in an extra deflection. In a non-linear analysis, the bending moments depend on the extra deflection of the column. An increase of the deflection results in an increase of the bending moments. Consequently, due to residual stresses the buckling load decreases.

It is very complicated to make calculations with the residual stress distribution in Figure 2.4. For simplicity another model for the stress distribution is adopted (Fig. 2.5). The value S is the amount of residual stress. The residual stress distribution in Figure 2.5 is a conservative approximation.

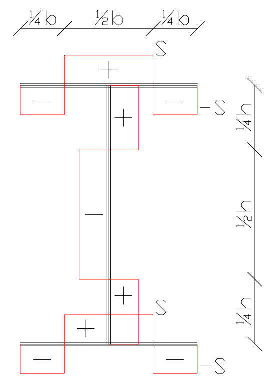

Figure 2.5: Residual stress distribution in a I section

The maximum deflection is in the midsection of the column. Therefore, the midsection is most loaded. The stresses in the midsection have been applied over the whole length of the column. This is a necessary approximation for performing the mathematical evaluations.

The considered section is a double symmetric HEA-section. The load is located in the centre of gravity. If one of the flanges partially yields and the other flange does not, the effective section is not double symmetric anymore. The effective centre of gravity has shifted. Due to extending the stress at midsection over the whole column, the centre of gravity in the whole column has shifted. To compensate this shift, an eccentric moment at both ends of the column has been introduced (Fig. 2.6). This eccentric moment results in an extra deflection. This extra deflection results again in an extra moment in the midsection (see App. C).

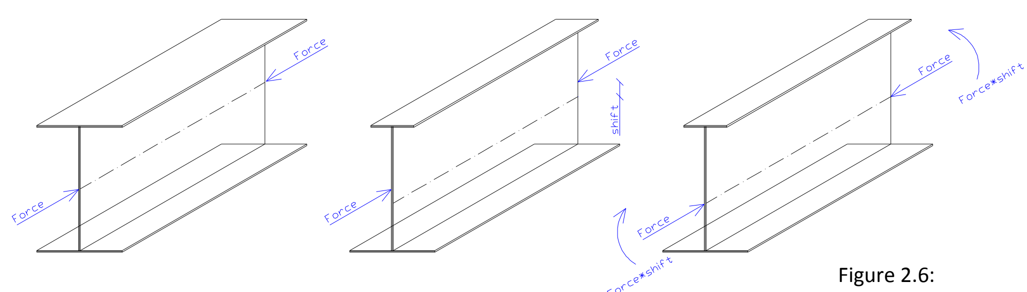

Figure 2.6: Eccentric moment

2.4 Calculation methods

There are many methods to calculate the deflection of a single column. The results of these methods can be found in the graph of Figure 2.7.

- First of all is the Euler buckling load (brown line). The deflection is zero till the Euler buckling load is reached. If the Euler buckling load is reached, the column fails and the deflection is undetermined.
- Secondly is the geometrical and physical linear (first order) analysis (blue line). This analysis results in a linear relation between the load and the deflection. The load is unlimited.
- As third, the geometrical non-linear and physical linear analysis (purple line). The total deflection is inversely proportional to the load. Limit of this analysis is the Euler buckling load.
- As fourth, the geometrical linear and physical non-linear analysis (red line). There is no deflection till the yield load is reached. The deflection at this load becomes infinity.
- As fifth, the geometrical and physical non-linear analysis (green line). This analysis contains both the yield load as well as the geometrical non-linear deflections.

The first part of the real load-deflection diagram (black line) follows the geometrical non-linear physical linear analysis.
After partial yielding, the deflection increases and the geometrical non-linear physical linear analysis is not valid anymore. The load increases till the ultimate load has been reached. The upper limit of the real load-deflection graph is the geometrical and physical non-linear analysis. There is no description or formula for the area between first yield and failure. In Appendix C an analysis is made to find a formula for this area. The analysis will be discussed in Section 2.6.

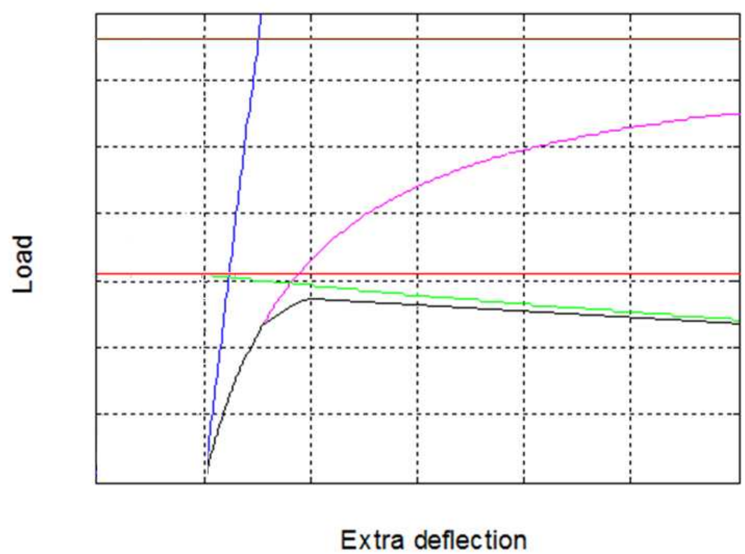

Figure 2.7:
Load-deflection diagram (schematic)

2.5 Failure

To calculate the failure load the stresses in the midsection must be calculated. The compression force results in compression stress in the whole midsection. The bending moment results in compression stress in the right flange and tension stress in the left flange. Due to the combination of the force and the moment the right flange yields first. After first yield, the half of the right flange cannot be used for the effective stiffness.

The Euler buckling load is the buckling load at ideal circumstances. The Euler buckling load is an upper limit of the real buckling load. The Euler buckling load can be calculated for the original section as well for the reduced section. If the section partially yields, the new upper limit is the Euler buckling load of the reduced section.

If right flange partially yields, there are three possible failure mechanisms (Figure 2.8 is a diagram of all failure mechanisms). These failure mechanisms are:

- The Euler buckling load of the reduced section is smaller than the load on the column. The reduced section cannot resist the load and the column buckle. The stiffness of the reduced section is too small (Fig. 2.9).
- The Euler buckling load of the reduced section is larger than the load on the structure and the load can increase. There are large deflections. This results in relative large bending moments. The right flange fully yields before the left flange starts to yield (Fig. 2.10). If one flange fully yields, the reduction of the stiffness and the eccentricity become too much. The column fails if the whole right flange yields.
- The Euler buckling load of the reduced section is larger than the load on the structure and the load can increase. The deflections are small so the bending moments are small too. The load increase till the left flange partial yields too. The effective section decreases again. The Euler buckling load can also be calculated for this reduced section. This possibility only occurs at a stiff section. The Euler buckling load of the reduced section is still smaller than the load on the column and the load can increases till the whole right flange yields (Fig. 2.11).

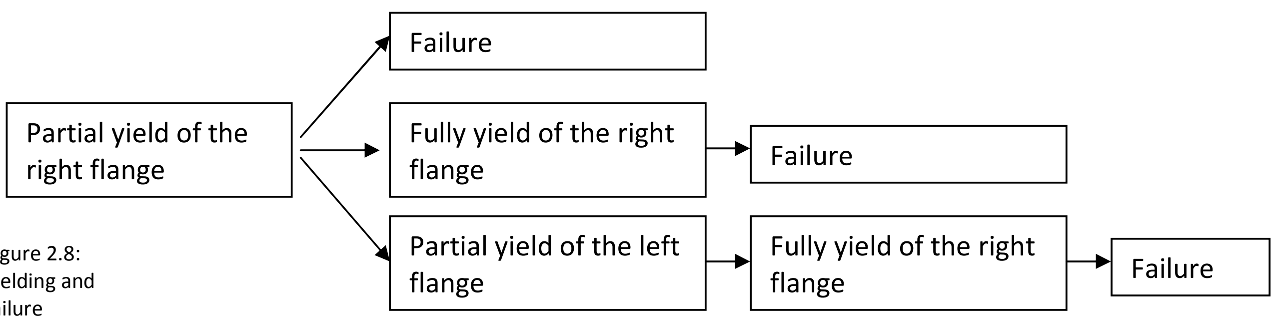

Figure 2.8: Yielding and failure

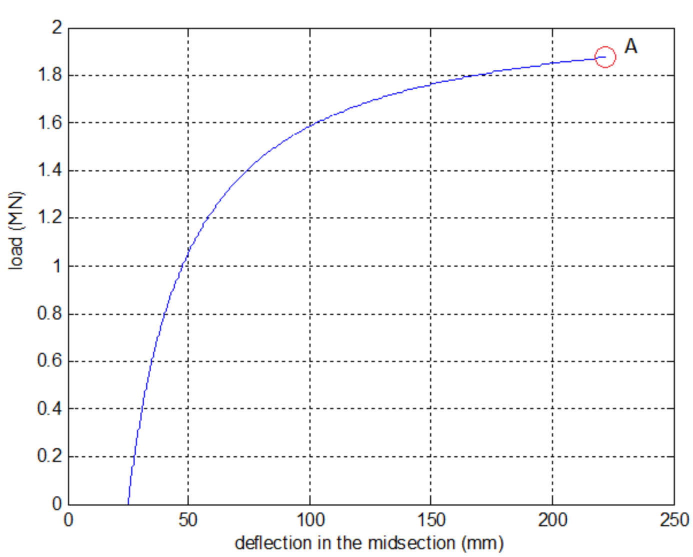

Calculation single column
Length: 25 m
HE 450A
S355
e_0 = 25 mm

Figure 2.9: Failure type 1

Figure 2.9 shows the deflection of the midsection of a column in the first failure type. The geometrical non-linear eccentricity has a major influence on the failure load. At a certain load (point A) the tips of the right flange starts to yield. The Euler buckling load of the reduced section is smaller than the load on the structure and the structure fails.

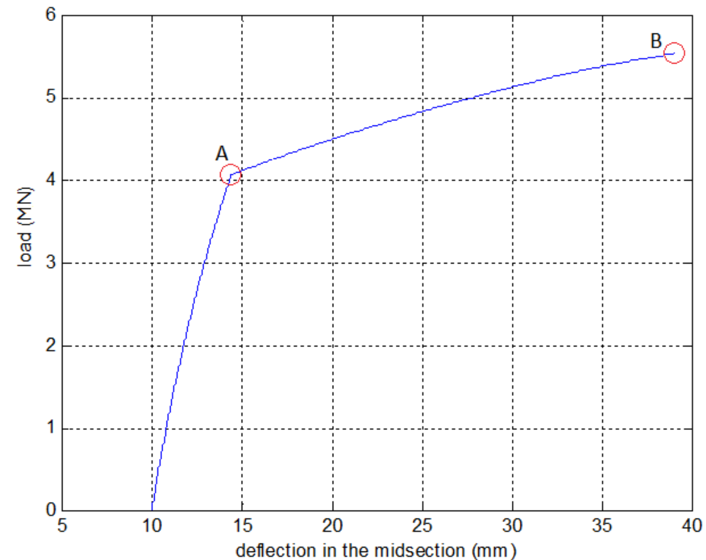

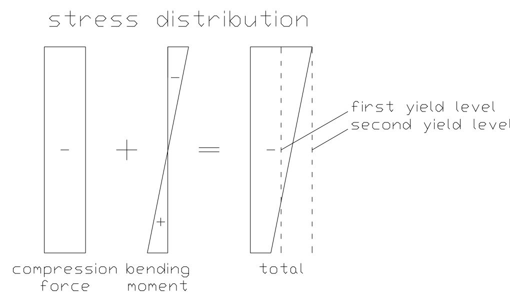

Calculation single column
Length: 10 m
HE 450A
S355
e_0 = 10 mm

Figure 2.10:
Failure type 2

Figure 2.10 shows the deflection of the midsection of a column in the second failure type. At a certain load (point A) the tips of the right flange starts to yield. The stiffness of the reduced section is large enough to resist more loads. The slope of the graph continues more slightly. At another load (point B) the whole right flange yields. This happens before the left flange starts to yield (see the stress distribution). If the whole right flange yields, the stiffness is reduced too much and the structure fails.

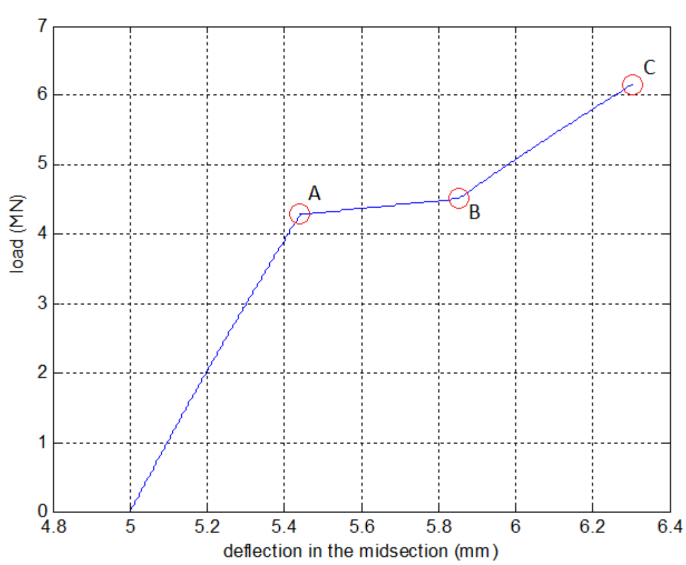

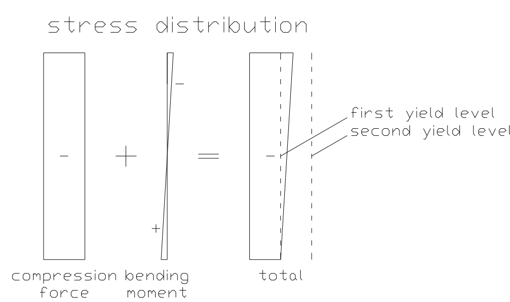

Calculation single column
Length: 5 m
HE 450A
S355
e_0 = 5 mm

Figure 2.11:
Failure type 3

Figure 2.11 shows the deflection of the midsection of a column in the third failure type. There are three interesting points in this graph. At point A the tips of the right flange start to yield. The stiffness reduces and the load increases till also the tips of the left flange start to yield (point B). The displayed stress distribution is the stress in point B. The load increase till the whole right flange yields and the structure fails.

For a better explanation of the load-deflection graph in the third failure possibility, several calculation methods are made (Fig. 2.12). Points A, B and C in figure 2.12 correspond to points A, B and C in figure 2.11. Figure 2.12 is a schematic load-deflection graph.

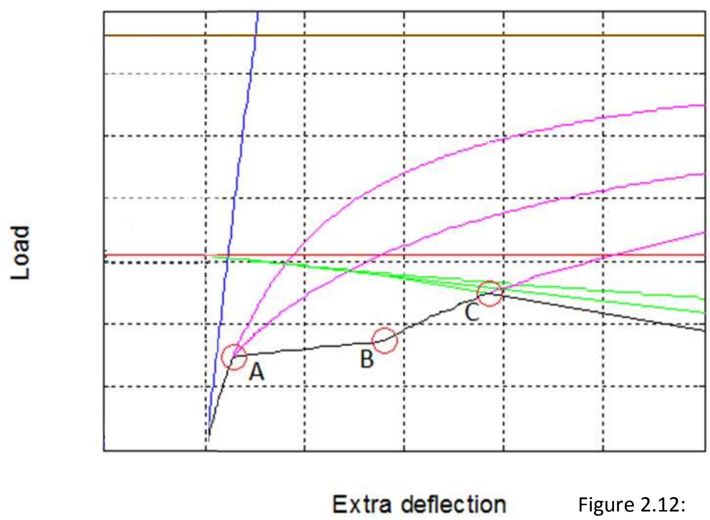

Figure 2.12: Load-deflection diagram (Schematic)

The first part of the load-deflection graph of the analysis (black line) is equal to the geometrical non-linear physical linear graph. If the tips of the right flange yields, the Euler buckling load of the effective section decreases. This results in a slighter geometrical non-linear graph. Due to the eccentric moments, the stresses and the deflection increase. The graph does not match with the geometrical non-linear graph. If the tips of the left flange yield too, the stiffness decrease and the geometrical non-linear graph become slighter again. The effective section is double symmetric again, so the eccentricity moments become zero. The graph match to the third geometrical non-linear graph till the failure load is reached.

The geometrical and physical non-linear calculation method (green line) is an upper limit of the failure load. If the deflection increases, the failure load decreases. Due to the yield steps, the slope of the geometrical and physical non-linear graph changes in points A and B. The third graph is the lowest upper limit of the ultimate load. The structure fails at point C.

2.6 Differential equation after first yield

The geometrical non-linear physical linear deflection formula (derived in Appendix A) is based on equilibrium between internal and external bending moments. The analysis in this Chapter is based on this equilibrium too. The difference between the geometrical non-linear physical linear calculation method and the analysis is the starting position.

To find a general formula, a general starting position must be taken. The starting position of the analysis is that the section partially yields. This starting position leads to the following starting points:

- There is an original load

- There is an original deflection
- There is a reduced section
- There is a shift in the centre of gravity

The internal and external bending moments of the original load case are in equilibrium. The equilibrium of the total internal and total external bending moments changes in the equilibrium between the increase of the internal and the increase of the external bending moments. The increase of the internal bending moment is the additional deflection multiplied by the reduced bending stiffness. The increase of the external bending moments is the original load multiplied by the additional deflection and the additional load multiplied by the total deflection.

With the equilibrium condition and the starting points an analysis can be made to calculate the total deflection. If the total deflection is known, the internal stresses and the ultimate load can be calculated. The method of calculation will be discussed in Section 2.7. A manual calculation and a computer-made calculation can be found in respectively Appendix D and Appendix E.

2.7 Calculation according to the analysis of Appendix C

In Appendix C a formula for the total deflection is derived. This formula is described in Section 2.6. The total deflection can be found by the following formula.

$$e_{total,i} = \frac{\left(F_{total,i-1} + F_i\right)\dfrac{F_i z_i L^2}{8EI_i} + \left(e_{total,i-1} + \dfrac{F_i z_i}{8EI_i}\right)F_{E,i} - e_{total,i-1}F_{total,i-1}}{F_{E,i} - F_{total,i-1} - F_i}$$

with:

$F_{total,i-1}$ is the original load

F_i is the increase of the load

z_i is the shift of the centre of gravity

$e_{total,i-1}$ is the total deflection at the original load ($F_{total,i-1}$)

$F_{E,i}$ is the Euler buckling load of the reduced section

The analyzed load case has subscript '*i*'. The total deflection depends on the original load, on the additional load and on the total deflection in the previous load case. The previous load case has subscript '*i*-1'. The original deflection in the first load case (*i*=1) is e_0. This is the initial deflection. There are no original loads or yielding parts in the first load case. Because of this, the formula can be simplified to:

$$e_{total,1} = \frac{e_0 F_{E,1}}{F_{E,1} - F_1}$$

The total deflection is a function of the load. The additional deflection and the bending moments are functions of the load too.

$$e_i = e_{total,i} - e_{total,i-1}$$

$$M_i = e_i F_{total,i-1} + e_{total,i} F_i$$

The stress in the flanges can be calculated by the following formulas:

$$\sigma_{right,i} = \sigma_{right,i-1} - \frac{F_i}{A_i} - \frac{M_i}{Z_i}$$

$$\sigma_{left,i} = \sigma_{left,i-1} - \frac{F_i}{A_i} + \frac{M_i}{Z_i}$$

The amount of residual stress does not change during the calculation. The compression stress increases if the load increases. The first load case ends if the tips of the right flanges start to yield. This happens if the summation of $\sigma_{right,1}$ and the residual stress reach the compression yield stress. The force that is necessary for this yielding is called F_1. If F_1 is known, the total deflection and the internal stresses can be calculated.

If the tips of the right flange yield, the effective cross-section decreases, the moment of inertia decreases and the centre of gravity shifts. The Euler buckling load can be calculated for the reduced section. If the Euler buckling load of this reduced section is larger than F_1 the load can increase. After yield of the tips of the right flange the second load case is started. The second load case ends if another part of the section starts to yield. The different failure possibilities are discussed in Section 2.5.

2.8 Calculation according to the Dutch Code

As a reference point, the Dutch Code is taken. The Dutch code is called the “TGB”, Technical foundation of build constructions (in Dutch: Technische grondslagen bouwconstructies). The most common building materials have their own part. One volume is about steel structures in general. The so called: the NEN 6770. The NEN 6771 and the NEN 6772 are respectively the requirements of steel stability and steel joints. The NEN 6770 and the NEN 6771 are used as reference points for the buckling calculations.

Both NEN 6770 and NEN 6771 include methods to calculate buckling loads. For a single column, supported at both ends and loaded by a compression force only, the calculation methods are the same. For other constructions or other loads, the calculation methods are different. This will be discussed in the chapter in question.

The buckling calculation method of the NEN 6771 is based on a unity check:

$$\frac{N_{c;s;d}}{\omega_{buc} N_{c;u;d}} \leq 1.0 \qquad \text{(art. 12.1.1.1).}$$

- $N_{c;s;d}$ is the maximum load on the column.
- $N_{c;u;d}$ is the yield load.
- ω_{buc} is the buckling reduction factor.

The buckling reduction factor (ω_{buc}) can be found by some stability curves (see App. B for the derivation). The buckling reduction factor depends on the relative slenderness, the length and the shape of the section.

2.9 *Calculation according to Matrix Frame*

Another possibility to calculate the ultimate load is the finite element method. There are many computer programs based on the finite element method. Matrix Frame is one of these computer programs. Matrix Frame is available for practical use and is specialized on frame type structures. To compare the buckling results, the calculations are also made with Matrix Frame.

Matrix Frame can calculate the ultimate load by a geometrical and physical non-linear analysis. The results of this calculation method should correspond with the NEN results and should correspond with the results of the analysis in Chapter two.

Matrix Frame has the possibility to calculate with straight sections only. Initial deflections must insert manually. A possibility to do so is to divide the column in small columns. All columns are fixed together and every joint has a horizontal displacement. All columns together illustrate the initial deflection.

Matrix Frame does not take residual stress into account. It is not possible to insert a section with different yield stresses. If the residual stress distribution of Figure 2.5 will be used the section must be divided in two equal parts. The section properties of these two parts separated must be equal to the half of the section properties of the original section. The influence of residual stress can be approached by using two different yield stresses. Three possibilities are made to calculate with two different sections.

The first possibility is to use two bars instead of one bar. Both bars have the same working line and the same deflection. The column should fail if both sections fail. The result of this calculation has not the desired effect. The buckling load is much lower than expected.

The second possibility is to make two calculations. The section parameters of all sections have been halved. The first calculation is the calculation with steel grade S235. The second calculation is the calculation with steel grade S460 (average yield stress is 347.5 N/mm^2). The section properties and the construction are the same in both calculations. In other words: the geometrical deflections are equal in both calculations. The only difference is the physical non-linear deflection. The graph of the geometrical and physical non-linear analysis is goes downwards (Section 2.4). According to this geometrical and physical non-linear analysis, the ultimate load decreases if the deflection increases. The decrease of the load can be calculated by the following formulas:

$M = wN$ (*w* is the deflection after reaching the ultimate load)

$\frac{M}{M_p} = 1.18\left(1 - \frac{N}{N_p}\right)$ (plastic behaviour of I sections)

$\Delta N = N_p - \frac{1.18 N_p M_p}{w N_p + 1.18 M_p}$ (ΔN is the decrease of the ultimate load)

The summation of the buckling load of both calculations is an upper limit for the real buckling load (Fig. 2.13). Figure 2.13 exists in three graphs. All graphs show the results of a geometrical and physical non-linear analysis. The third graph is the summation of first and the second. It is clear that the deflection of point A is not equal to the deflection of point C. The ultimate load according to this calculation possibility is the summation of point A and C. The 'real' buckling load is the summation of point B and C. There are small differences between these values.

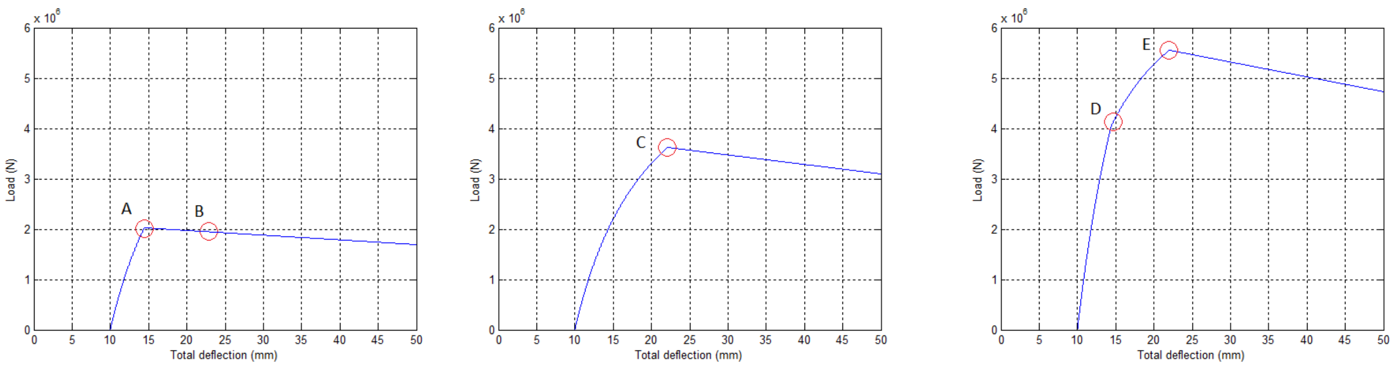

Figure 2.13: Load-deflection diagrams

Figure 2.14 is the ultimate load distribution for different possibilities to take residual stress into account.

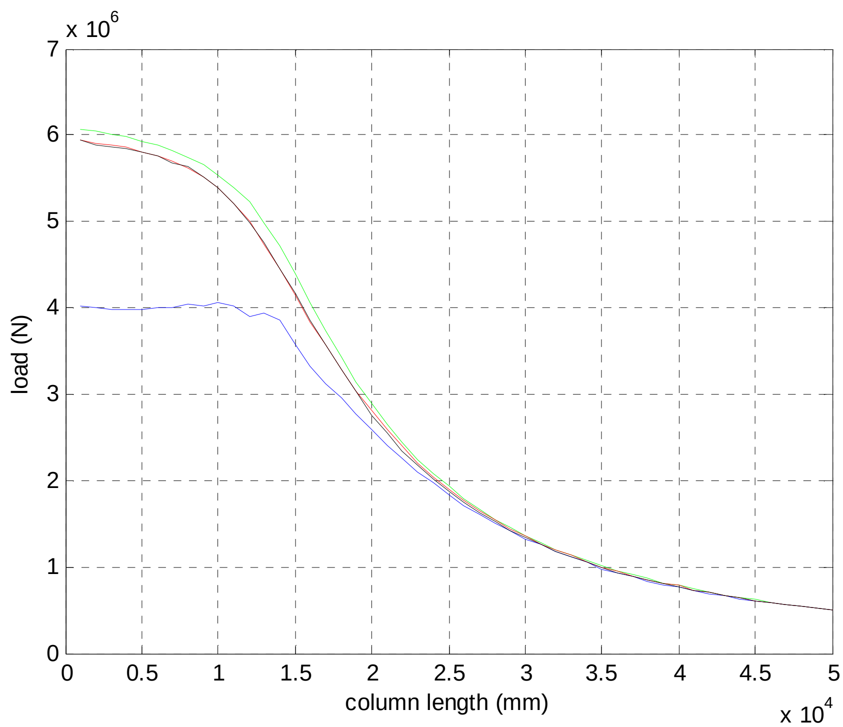

Figure 2.14: Load-deflection diagram

- Buckling load without residual stress (green line)
- Buckling load with two bars on the same working line (blue line)
- Buckling load with two separate calculations (red line)

The black line is discussed later on.

Interesting is the graph for the buckling load with two bars on the same working line. This graph shows a weird change of direction. In this calculation method, the buckling load of non-slender structures decreases enormously. The buckling load of slender structures depends mainly on the Euler buckling load. The yield stress has hardly any influence on the failure load. The results of all Matrix Frame calculations are close together.

The ultimate load on non-slender structures corresponds with the yield load of the lowest yield stress. Only one statement is found to explain what happens. Matrix Frame calculates with two bars with an infinity small distance to each other. Matrix frame divides the load in two equal parts. Both bars are loaded equally. After partial yielding, the moments will be re-distributed. There is no re-distribution of the compression force. The load increases till one section carries all bending moments and the other section is fully yield in compression. If a section fully yields, all stiffness is lost. The structure cannot resist more loads and the structure becomes unstable. The load on the column has reached the limit.

The problem of the non-slender structures can be found in the distribution of the normal forces. The problem can be solved by distribute the normal force manually. This can be done by using two columns with the same initial deflection and the fixed distance between (third possibility). The distance can be kept fixed by using hinged struts between the columns. The load on the bar with steel grade S235 is $\frac{235}{695}$ of the total load and the load on the bar with steel grade S460 is $\frac{460}{695}$ of the total load. The total load is properly distributed over the yield stresses. Different loads result in different deformations. Due to the hinged struts between the columns, the deflections of both columns are equal. The elongation of the column has no influence on the buckling calculation of a single column. The only point of attention is the distance between the columns. Matrix Frame cannot find equilibrium in elongation if the distances between the columns are too short.

With this calculation method, the buckling load can be calculated. The results are displays in Figure 2.14 too (black line). The results of this calculation method are very close to the calculation method of using two calculations (second possibility). For the comparison of the buckling load of a single column the third possibility is used. For the calculation of the ultimate load of a portal frame (Chapter three and Chapter four) the second calculation possibility is used.

2.10 Conclusions
Chapter two was about buckling of a single column. A column loaded by a centric normal force can deflect because of the shape imperfections of the column and the residual stress in the column. Different methods have been used to calculate the buckling load of a single column. The results are shown as stability curves in Figure 2.15 (page 20).

The Euler buckling load is the buckling load of an ideal column. An ideal column is perfectly straight, homogeneous and free of residual stresses. In practice an ideal column does not exist. The Euler buckling load is an upper limit of the real buckling load (black curve).

The buckling load can be calculated by formulas in the Dutch code (NEN 6771). The NEN 6771 is used in the whole of the Netherlands and can be used as referential point for other calculation methods (red curve).

The Matrix Frame calculation is based on the finite element method. Matrix Frame does not automatically include initial deflections or residual stresses. The initial deflection and the residual stresses must be inserted manually.

The column can be divided in small columns. All of these columns are fixed together. The joints of the columns have a (different) horizontal displacement. Using this, the shape imperfections can be introduced.

The residual stress can be introduced by splitting the column into two columns. The separated columns are connected by hinged struts. These struts are used to obtain the same deflections in both columns. The section properties of each separated column must be equal to the half of the section properties of the original section. The steel grades of the two columns must be different (one column steel grade S235 and one column steel grade S460, average 347.5). The loads on the column must be distributed over the columns in proportion to the yield stresses. The buckling load can be calculated by a geometrical and physical non-linear analysis. The result of the Matrix Frame calculation is the green curve in Figure 2.15.

A non-linear analysis is made to find a formula for the total deflection of the column. The total deflection is necessary to calculate the buckling load. The following formula is the result of the differential equation.

$$e_{total,i} = \frac{\left(F_{total,i-1} + F_i\right)\dfrac{F_i z_i L^2}{8EI_i} + \left(e_{total,i-1} + \dfrac{F_i z_i}{8EI_i}\right)F_{E,i} - e_{total,i-1}F_{total,i-1}}{F_{E,i} - F_{total,i-1} - F_i}$$

The index '*i*' corresponds to the i^{th} load case. The index '*i*-1' corresponds to the load on the column before the i^{th} load case starts. Force F_{i-1} results to yielding in a part of the section. The result of the formula ($e_{total,i}$) is the total deflection in the i^{th} load case.

To calculate the buckling load, not only the total deflection has to be calculated, but also the stresses in the section. The stresses can be calculated by the following formulas.

$$e_i = e_{total,i} - e_{total,i-1}$$

$$M_i = e_i F_{total,i-1} + e_{total,i} F_i$$

$$\sigma_{top,i} = \sigma_{top,i-1} - \frac{F_i}{A_i} - \frac{M_i}{Z_i}$$

$$\sigma_{bottom,i} = \sigma_{bottom,i-1} - \frac{F_i}{A_i} + \frac{M_i}{Z_i}$$

It is possible to take the residual stress into account with these formulas. The buckling load can be calculated by the following steps.

a) The first yield point must be found.
b) Stress in right flange and in left flange must be calculated

c) Calculated a reduced Euler buckling load for the reduced section
d) The next yield point must be calculated
e) Repeat step b and c till the Euler buckling load of the reduced section is lower than the load on the structure

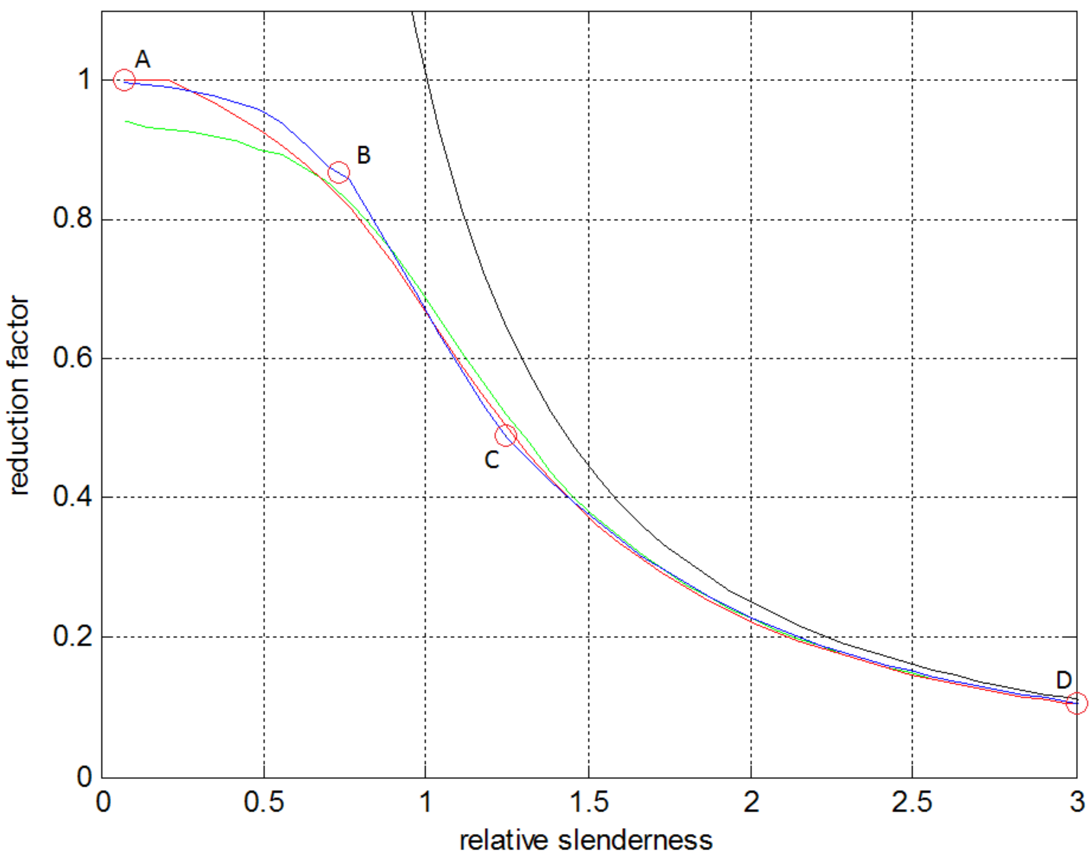

Figure 2.15:
Stability curve for several calculations methods

For four different calculation methods the stability curve is drawn.
These curves can be found in Figure 2.15. The calculation methods are:

- The black curve is the load according to Euler
- The red curve is the load according to the Dutch code
- The green curve in the load according to the Matrix Frame
- The blue curve is the load according to the analysis in Appendix C

The Euler buckling load is the upper limit of the real buckling load. The stability curve of all other buckling calculations is smaller. The upper limit is not exceeded.

The results of the Matrix Frame calculations for non-slender structures are very conservative. According to the Matrix Frame calculation, a non-slender structure will never reach the yield load. The buckling loads according to the Dutch code and the results of the analysis in Appendix C are more realistic for non-slender structures.

The curve according to the analysis in Appendix C (blue curve) is divided in three parts. The stiffness of the first part (part AB) is large. Also the reduced stiffness (after partial yielding) is large enough to resist the loads. The deflections are small. The whole right flange and the half of the left flange yields before the column fail. The deflections in the second part (part BC) are larger than the deflections in part AB. In this second part, the left flange does not yield. The column fails if the right flange fully yields. The columns in the third part of the curve (part CD) are slender. The stiffness of the reduced section is too small to resist more loads and the column fails if the right flange partial yields.

Chapter 3 Unbraced Portal Frame

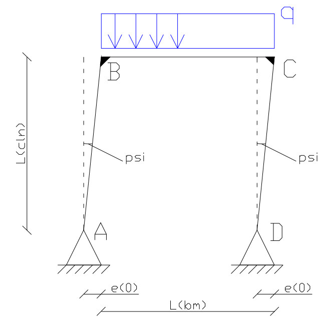

Figure 3.1: Structure

In this chapter an unbraced Portal Frame will be analysed (Fig. 3.1). The portal frame system includes two column sections and one rafter section. The columns are supported by two hinges. The frame is loaded by a uniformly distributed vertical load on the rafter. Self-weight has been neglected.

3.1 Structure

As discussed in Chapter 2.2 a section has an initial deflection due to the production. This initial deflection is idealised as a half sine function shape. Beside production imperfections there are also construction imperfections. The construction imperfection of an unbraced structure is an angle between the designed structure and the real structure (Fig. 3.1). According to the NEN 6771 (art. 10.2.5) this angle (ψ) is 0.004 rad. Clearly, due to construction imperfections the structure is not symmetrical.

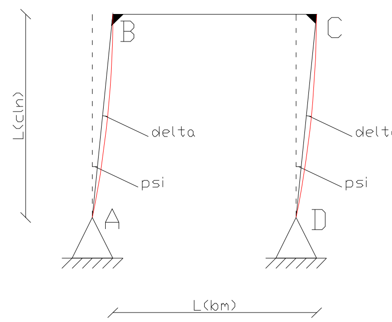

Figure 3.2: Imperfections

The influence of the construction imperfections is larger than the influence of the production imperfections. Figure 3.2 shows the production imperfections and the construction imperfections in one structure. Due to the production imperfections the bending moments in the middle of the columns increase. The bending moments in point B and in point C do not change due to the production imperfections. The bending moments in these points are larger than the bending moments in the middle of the column. In practice, the influence of the production imperfections is taken into account by applying the governing code equations. The construction imperfections are taken into account by manually adding them to the frame model.

The analysis in this Chapter (App. H till K) is based on the failure mechanism of the columns. It is assumed that the columns are critical. Lateral buckling or other failure mechanisms in the beam has been ignored. This assumption has been checked afterwards.

Due to asymmetry of the portal frame, the bending moment in point C is larger than the bending moment in point B. Column CD is heavier loaded than column AB. Column CD fails first. The analysis in this Chapter is based on the failure mechanism of column CD. The structure is a statically indeterminate structure to the first degree. The portal frame fails if two parts of the structure yield. The first part is joint C and the second part is joint B. It is assumed that the structure fails if the right hand column fails at joint C.

3.2 Different types of analysis

In this section four analyses are made (see also Section 2.4).

- Geometrical linear analysis
- Geometrical linear analysis with residual stress

- Geometrical non-linear analysis
- Geometrical non-linear analysis with residual stress

The easiest analysis is the geometrical linear analysis without residual stress (App. H). This analysis assumes in a linear relation between the deflection and the load. The deflection of the portal frame does not influence the reaction forces. The graph of this analysis can be limited by the plastic collapse load. This results in a bi-linear load-deflection graph.

A little bit more difficult is a geometrical linear analysis where residual stress is taken into account (App. I). At a certain load, one of the columns will partial yield. The stiffness of this column decreases and the deflection increase. At a second load another part of the section starts to yield. The deflection increases again. The failure mechanism depends on the section properties and the lengths. The different failure mechanisms are discussed in Section 2.5. The linear analysis is made to better understand the non-linear analyses.

In a geometrical linear analysis the deflections do not influence the reaction forces. In a geometrical non-linear analysis the deflections do influence the reaction forces. The total deflection influences on the internal stresses. If the deflection increases, the internal moments increase. If the moments increase, the ultimate load decreases. In Appendix J, the geometrical non-linear analysis for the portal frame is calculated without influence of residual stress. Residual stress is taken into account in the analysis of Appendix K. The formulas as results of the analysis in Appendix K are very complex. Computer programs like Excel or MatLab must be used to make calculations with these formulas.

3.3 Calculation method

The portal frame is loaded by a uniformly distributed load. The load results in bending moments and in normal forces. It is assumed that the beam will not fail. The column is critical. The largest moment in the column is the moment at the end of the column. This moment depends mainly on the deflection of the column. The deflection that will be calculated is the deflection in point C. This is not the maximum deflection (Fig. 3.3). The location of the maximum deflection is not constant. It is not necessary to calculate the maximum deflection and the location of the maximum deflection because this is not the critical cross-section. The critical cross-section is point C.

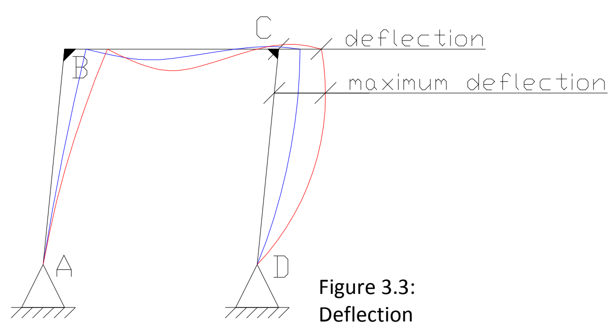

Figure 3.3: Deflection

The total deflection depends on the stiffness of the beam and the stiffness of the column. The total deflection has been split is two parts. The first part depends on the beam and the second part depends on the column.

The beam is loaded by a uniformly distributed load and a bending moment at both ends of the beam. Due to this load, the beam deflects and rotates. The rotation at the end of the beam is the same as the rotation of the end of the column. The deflection of the column is the multiplication of the rotation at the end and the column length. This part of the deflection depends on the stiffness of the beam.

The second part of the deflection depends on the column. Both ends of the column have a degree of freedom. One end of the column is connected to the beam. The rotation is limited by the beam. The rotation of the beam is already taken into account at the first part of the deflection. The beam is not supported horizontally. The horizontal displacement of the beam is only limited by the column. The other end of the column is the support. The support is a hinge and can rotate freely. The support cannot displace. Both ends together can be schematized as a cantilever beam with a free end (Fig. 3.4). The loads on this cantilever beam are the reaction forces of the support. The portal frame is out of square. In other words: the horizontal and vertical reaction forces are not perpendicular or parallel to the working line of the cantilever beam. A remaining force perpendicular to the cantilever beam is introduced. This remaining force depends on the reaction forces and the total deflection.

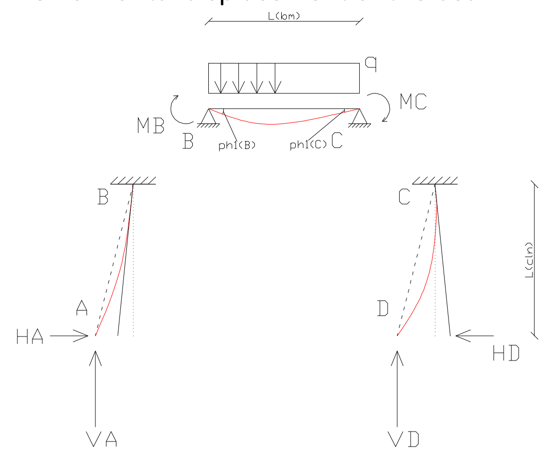

Figure 3.4: Deflections

The total deflection of column AB and the total deflection of column CD can be calculated. Both columns are part of one structure. The difference in deflection is the elongation of the beam. The elongation of the beam is very small compare to the deflection of the columns and can be neglected. In other words: the deflection of column AB is equal to the deflection of column CD. This equilibrium is the basic of the analyses in Appendices H, I, J and K.

3.4 Calculation according to the analysis of Appendices J and K

As discussed before four analyses have been made. Two geometrical linear analyses and two geometrical non-linear analyses. These analyses can be found in appendices H till K. The physical properties result in an upper limit of the load. The geometrical non-linear analyses are closest to reality. Because of this, the geometrical non-linear analyses are most interesting. The geometrical linear analyses are made to better understand the geometrical non-linear analyses. The geometrical linear and the geometrical non-linear analyses have the same starting point.

The calculation method is discussed in Section 3.3. All analyses are based on transversal and rotation equilibrium conditions and on equilibrium in the deflection of the columns. In the geometrical linear analyses the deflections do not have any influence on the moment distribution in the structure. In the geometrical non-linear analyses the deflections do influence the moment distribution. Because of this influence the analyses and the formula become very complex.

Two geometrical non-linear analyses are made. One with and one without residual stress. The analysis with residual stress is divided in two parts. In total there are three sets of formulas to calculate the ultimate load. The different parts correspond to the yield parts.

The first set of formulas can be used to calculate the deflections and the stresses till the section starts to yield. Due to the combination of a compression force and a positive bending moment, the right flange of the section yields first.

The second part can be used if the right flange partial yields and the stiffness of the reduced section is large enough to resist more loads. The stiffness of the reduced section is large enough if the denominator of the formula to calculate the additional deflection results in a positive value. In this part also the shift of the centre of gravity in the effective section must be taken into account. The second part ends if the left flange partial yields too or the right flange fully yields.

The third part can only be used if both flanges partial yield and the stiffness is large enough to resist more loads. In the most calculations the third part does not occur. In the third part, the midsection of the column has changed in a symmetric section. Due to the generalisation of the stress, the whole section is symmetric. The load is located in the effective centre of gravity again.

It is important to know that one column is heavier loaded than the other column. Due to this difference only one column will (partial) yield. The stiffness of only one column decreases. The stiffness of the other column remains constant.

The following formulas can be used to calculate the reaction forces, the bending moments and the additional deflections in several load cases.

The first load case:

$$V_{D,1} = q_1\left(\tfrac{1}{2}L_{bm} + e_{total,1}\right)$$

$$V_{A,1} = q_1\left(\tfrac{1}{2}L_{bm} - e_{total,1}\right)$$

$$M_{B,1} = q_1\left(\tfrac{1}{2}L_{bm} - e_{total,1}\right)e_{total,1} - H_{A,1}L_{cln}$$

$$M_{C,1} = q_1\left(\tfrac{1}{2}L_{bm} + e_{total,1}\right)e_{total,1} + H_{A,1}L_{cln}$$

$$e_{total,1} = \frac{12\psi L_{cln}EI_{bm}EI_{cln,1}}{12EI_{bm}EI_{cln,1} - q_1L_{bm}{}^2L_{cln}EI_{cln,1} - 2q_1L_{bm}L_{cln}{}^2EI_{bm}}$$

$$H_{A,1} = q_1\frac{L_{bm}{}^3L_{cln}EI_{cln,1}}{12L_{bm}L_{cln}{}^2EI_{cln,1} + 8L_{cln}{}^3EI_{bm}} - qL_{cln}\left(\frac{12\psi EI_{bm}EI_{cln,1}}{12EI_{bm}EI_{cln,1} - q_1L_{bm}{}^2L_{cln}EI_{cln,1} - 2q_1L_{bm}L_{cln}{}^2EI_{bm}}\right)^2$$

The second load case:

$$V_{D,2} = q_1e_2 + q_2\left(\tfrac{1}{2}L_{bm} + e_1 + e_2\right)$$

$$V_{A,2} = -q_1e_2 + q_2\left(\tfrac{1}{2}L_{bm} - e_1 - e_2\right)$$

$$M_{C,2} = q_2\left(\tfrac{1}{2}L_{bm} + e_1 + e_2\right)\left(e_1 + e_2 + z_2\right) + q_1e_2\left(\tfrac{1}{2}L_{bm} + 2e_1 + e_2 + z_2\right) + H_{A,2}L_{cln}$$

$$M_{B,2} = q_2\left(\tfrac{1}{2}L_{bm} - e_1 - e_2\right)\left(e_1 + e_2\right) + q_1e_2\left(\tfrac{1}{2}L_{bm} - 2e_1 - e_2\right) - H_{A,2}L_{cln}$$

$$H_{A,2}=\frac{\begin{pmatrix}-q_{total,2}L_{bm}L_{cln}e_2\left[12e_2+24e_1+8z_2+2L_{bm}\right]EI_{cln,2}+q_{total,2}L_{cln}{}^2e_2\left[4L_{bm}-16e_1-8e_2\right]EI_{bm}\\+24e_2EI_{bm}EI_{cln,2}+q_2L_{bm}L_{cln}\left[L_{bm}{}^2-2L_{bm}e_1-12e_1{}^2-4L_{bm}z_2-8e_1z_2\right]EI_{cln,2}-q_2L_{cln}{}^2e_1\left[4L_{bm}+8e_1\right]EI_{bm}\end{pmatrix}}{12L_{bm}L_{cln}{}^2EI_{cln,2}+8L_{cln}{}^3EI_{bm}}$$

$$e_2=\frac{q_2L_{bm}L_{cln}\begin{bmatrix}6L_{bm}{}^2e_1EI_{cln,1}EI_{cln,2}+3L_{bm}{}^2z_2EI_{cln,1}EI_{cln,2}+6L_{bm}e_1z_2EI_{cln,1}EI_{cln,2}\\+8L_{bm}L_{cln}e_1EI_{bm}\left(EI_{cln,1}+EI_{cln,2}\right)+L_{bm}{}^2L_{cln}EI_{bm}\left(EI_{cln,1}-EI_{cln,2}\right)+8L_{cln}{}^2e_1\left(EI_{bm}\right)^2\\+2L_{cln}z_2\left(L_{bm}+2e_1\right)EI_{bm}\left(-EI_{cln,1}+2EI_{cln,2}\right)\end{bmatrix}}{2\begin{bmatrix}-3q_{total}L_{bm}{}^3L_{cln}EI_{cln,1}EI_{cln,2}-3q_{total}L_{bm}{}^2L_{cln}z_2EI_{cln,1}EI_{cln,2}\\-4q_{total}L_{bm}{}^2L_{cln}{}^2EI_{bm}\left(EI_{cln,1}+EI_{cln,2}\right)-2q_{total}L_{bm}L_{cln}{}^2z_2EI_{bm}\left(-EI_{cln,1}+2EI_{cln,2}\right)\\-4q_{total}L_{bm}L_{cln}{}^3\left(EI_{bm}\right)^2+12L_{cln}\left(EI_{bm}\right)^2\left(EI_{cln,1}+EI_{cln,2}\right)+36L_{bm}EI_{bm}EI_{cln,1}EI_{cln,2}\end{bmatrix}}$$

The third load case:

$V_{D,3}=e_3\left(q_1+q_2\right)+q_3\left(\tfrac{1}{2}L_{bm}+e_1+e_2+e_3\right)$

$V_{A,3}=-e_3\left(q_1+q_2\right)+q_3\left(\tfrac{1}{2}L_{bm}-e_1-e_2-e_3\right)$

$M_{C,3}=e_3\left(q_1+q_2\right)\left(\tfrac{1}{2}L_{bm}+2e_1+2e_2+e_3\right)+q_3\left(\tfrac{1}{2}L_{bm}+e_1+e_2+e_3\right)\left(e_1+e_2+e_3\right)+H_{A,3}L_{cln}$

$M_{B,3}=e_3\left(q_1+q_2\right)\left(\tfrac{1}{2}L_{bm}-2e_1-2e_2-e_3\right)+q_3\left(\tfrac{1}{2}L_{bm}-e_1-e_2-e_3\right)\left(e_1+e_2+e_3\right)-H_{A,3}L_{cln}$

$$H_{A,3}=\frac{\begin{pmatrix}-q_{total,3}L_{bm}L_{cln}\left[2L_{bm}e_3+24e_1e_3+24e_2e_3+12e_3{}^2\right]EI_{cln,3}\\-q_{total,3}L_{cln}{}^2\left[4L_{bm}e_3+16e_3e_1+16e_3e_2+8e_3{}^2\right]EI_{bm}\\+q_3L_{bm}L_{cln}\left[L_{bm}{}^2-2L_{bm}e_2-2L_{bm}e_3-12e_1{}^2-24e_1e_2-12e_2{}^2\right]EI_{cln,3}\\-q_3L_{cln}{}^2\left[4L_{bm}e_1+4L_{bm}e_2+8e_1{}^2+16e_1e_2+8e_2{}^2\right]EI_{bm}+24e_3EI_{bm}EI_{cln,3}\end{pmatrix}}{12L_{bm}L_{cln}{}^2EI_{cln,3}+8L_{cln}{}^3EI_{bm}}$$

$$e_3=\frac{q_3L_{bm}L_{cln}\begin{bmatrix}6L_{bm}{}^2\left(e_1+e_2\right)EI_{cln,1}EI_{cln,3}+8L_{bm}L_{cln}\left(e_1+e_2\right)EI_{bm}\left(EI_{cln,1}+EI_{cln,3}\right)\\+8L_{cln}{}^2\left(e_1+e_2\right)\left(EI_{bm}\right)^2+L_{bm}{}^2L_{cln}EI_{bm}\left(EI_{cln,1}-EI_{cln,3}\right)\end{bmatrix}}{2\begin{bmatrix}-3L_{bm}{}^3L_{cln}q_{total}EI_{cln,1}EI_{cln,3}-4L_{bm}{}^2L_{cln}{}^2q_{total}EI_{bm}\left(EI_{cln,1}+EI_{cln,3}\right)-4L_{bm}L_{cln}{}^3q_{total}\left(EI_{bm}\right)^2\\+36L_{bm}EI_{bm}EI_{cln,1}EI_{cln,3}+12L_{cln}\left(EI_{bm}\right)^2\left(EI_{cln,1}+EI_{cln,3}\right)\end{bmatrix}}$$

An example of the total deflection of the non-linear analysis is shown in Figure 3.5.

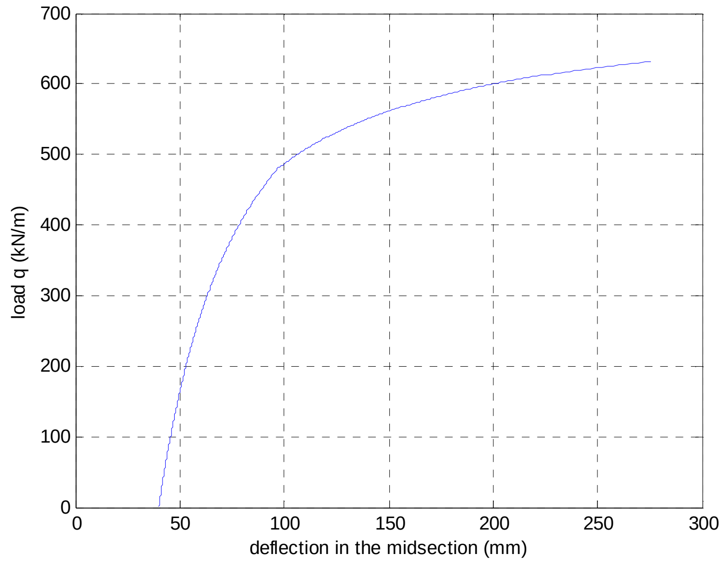

Calculation unbraced portal frame

Column:	Length: 10 m HE 360A
Beam:	Length: 5 m HE 900A

S355
e_0 = 40 mm

Figure 3.5: Load-deflection graph

3.5 Calculation according to the Dutch code

In Section 2.8 a buckling calculation of a single column is made according to the Dutch code (NEN 6771). This code also contains a calculation method for the ultimate load calculation for the column of a portal frame. If the portal frame is only loaded by a vertical point load on each column, the ultimate load calculation of an unbraced portal frame is almost the same as the buckling calculation of a single column. The only difference is the buckling length. In this study is chosen for a uniformly distributed load on the beam. This load results in compression forces and in bending moments. The formula to calculate the buckling load for a structure with a point load only is not valid anymore. Another formula must be used. A linear analysis must be made to transform the uniformly distributed load in point loads and bending moments. With these values a code check can be made.

A very important issue to calculate the ultimate load is the buckling length. The buckling length of the column of the portal frame depends (beside the length of the column) on two aspects.

- First (at the most important) is the type of the portal frame. Is the portal frame braced or not. The buckling length of a braced portal frame is maximum the column length. The buckling length of an unbraced portal frame is at least twice the column length.
- Second the buckling length depends on rotation freedom. The rotation freedom depends on the stiffness of the column, the stiffness of the beam and the type of support.

After a linear analysis, the column of the portal frame can be schematized as a single column (with a buckling length instead of a system length) loaded by a normal force and a bending moment. Because of the presence of the bending moments, the formula for the buckling load in Chapter two is not valid anymore. The following formula must be used.

$$\frac{N_{c;s;d}}{N_{c;u;d}} + \frac{n_y}{n_y - 1} \frac{M_{y;equ;s;d} + N_{c;s;d} e_y^*}{M_{y;u;d}} \leq 1.0$$ (NEN 6771 art. 12.3.1.2.1)

In this formula is:

$N_{c;s;d}$, $M_{y;equ;s;d}$	The loads on the column
$N_{c;u;d}$	Plastic normal force
n_y	Relation between the Euler buckling load and the load on the structure (Note: for the Euler buckling load, the buckling length must be taken)
$M_{y;u;d}$	Plastic bending moment
e_y^*	Imperfection parameter

e_y^* must be calculated by the following formula:

$$e_y^* = \alpha_k \left(\lambda_{y;rel} - \lambda_0\right) \frac{M_{y;u;d}}{N_{c;u;d}}$$

3.6 Calculation according to Matrix Frame

Matrix Frame has been used to calculate the failure load of an unbraced portal frame. The beam has been made strong enough to be sure that the column is critical. The columns of the portal frame have been split in four points. For the calculation it is not necessary to split the column in parts. This has been done to get a better understanding on the deflections and the moment distribution. Using small elements, the maximum deflection and the maximum bending moment can be found easily. As discussed before the maximum bending moment is at the end of the column and the location of the maximum deflection is variable. The calculation file of Matrix Frame can be found in Appendix L.2.

In Section 2.9 three calculation methods have been discussed to take care of the residual stress. One problem is the amount of residual stresses. In Chapter two a HE 450A section is chosen to calculate the ultimate load. The amount of residual stress in this section is 30% of the yield stress. For the calculations in this Chapter a HE 360A section is chosen. This section is chosen to be sure that the column is critical. A heavier column results in failure of the beam. The amount of residual stress in this section (50% of the yield stress) is larger than the amount of residual stress in a HE 450A section. For a better result the stresses in Matrix Frame the yield stress must be changed. This is not possible. As comparison the amount of residual stress of 30% is taken to calculate the ultimate load by Matrix Frame. The differences will be discussed in Section 3.7.

In the calculation of the single column, the first calculation method did not result in correct values. This calculation method will not be discussed in this Chapter.

The second calculation method was to bisect the section properties of all elements. The calculation is made twice. The steel grade of the first calculation is S235 and the steel grade of the second calculation is S460. (For a real comparison the yield stresses must be 177 N/mm^2 and 532 N/mm^2). The summation of these calculations is the ultimate load. The sections and the loads at both calculations are the same, so the geometrical deflections are equal in both calculations. According to the geometrical and physical non-linear analysis, the ultimate load decreases if the deflection increases. This can result in differences in the total ultimate load. The real ultimate load is slightly less that the ultimate load calculated by this method. In Section 2.9 is proofed that these differences are negligible.

The third calculation method was to split the sections and connect the sections with a hinged strut. The total load must be properly distributed over the yield stresses. For a single column it was relative easy to distribute the load. It is very complicated to distribute the loads of a portal frame. Two portal frames must be made. Using hinged struts the normal forces can be divided properly. The bending moments depends on the loads and on the deflections. The deflections in both sup-structures are equal. The distribution of the bending moments cannot be steered easily.

It is very complicated to get proper results of the third calculation method. The second calculation method has been used to calculate the ultimate load.

Figure 3.6 shows two load-deflection graphs. The blue curve is the calculation without residual stress. The red curve is the calculation with residual stress (according to the second calculation method).

The curve with residual stress is lower than the curve without residual stress. For slender structures these differences are very small. For non-slender structures the difference is about five percent. The curve with residual stress will be used to compare with other calculation methods.

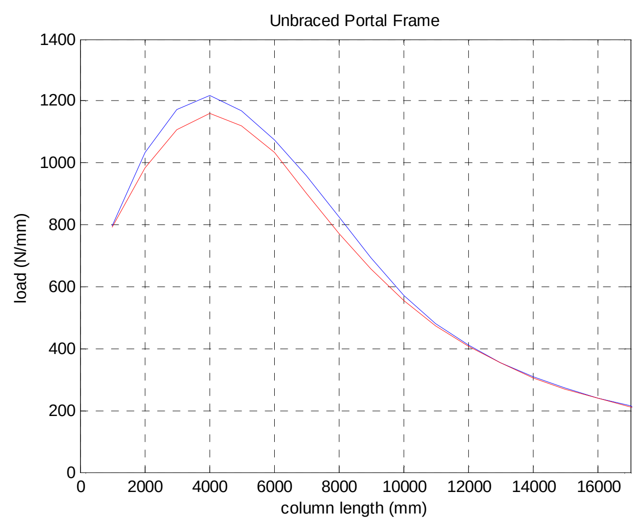

Figure 3.6: Load-deflection graphic

3.7 Conclusions
Chapter three was related to an unbraced portal frame. The ultimate load has been calculated by three calculation methods. The results of the calculations are expressed in a load-deflection graph (Fig. 3.7).

An analysis is made to find three sets of formulas to calculate the additional deflection. These sets correspond to different yield phases of the structure. These formulas can be used to calculate the ultimate load. This calculation method is the blue curve in Figure 3.7.

To calculate the ultimate load according to the Dutch code (red curve) a linear analysis must be made. The uniformly distributed load must be transform to normal forces and bending moments. These values can be used as input for the unity checks.

The Matrix Frame calculation is divided in two parts. Both parts have a different yield stress. Both parts together illustrate the residual stress. The real amount of stress cannot be schematized in Matrix Frame. The result of this calculation method is the green curve in Fig. 3.7.

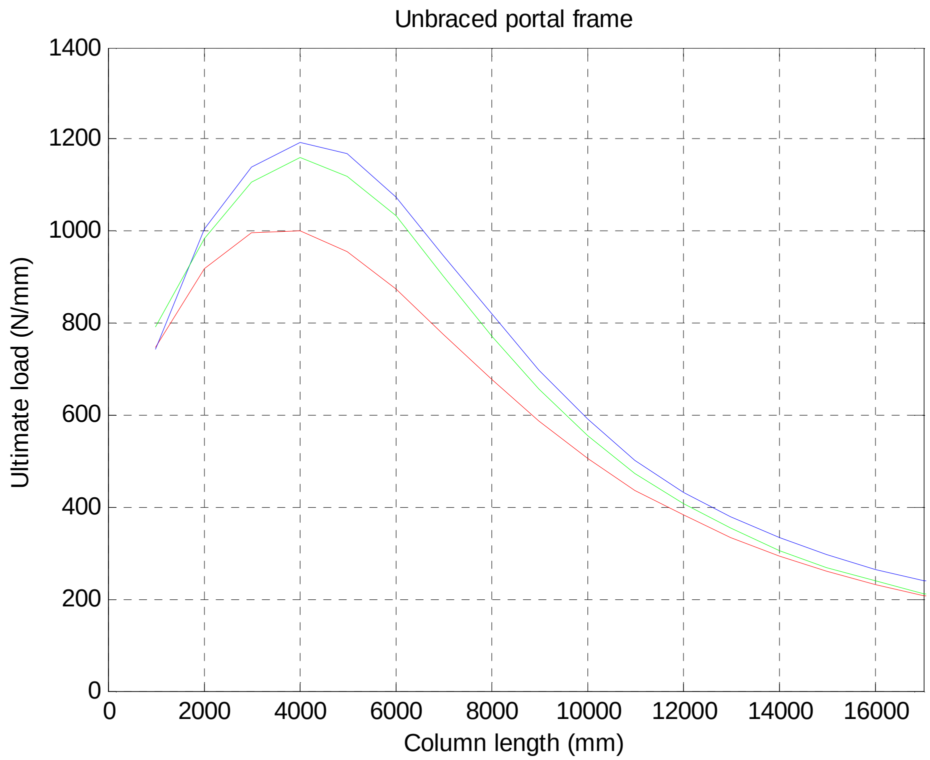

Calculation unbraced portal frame

Column:
Length: variable
HE 360A
Beam: Length: 5 m
HE 900A

S355

Figure 3.7: Load-deflection graphs

- The red curve is the load according to the Dutch code
- The green curve in the load according to the Matrix Frame
- The blue curve is the load according to the analysis in Appendices J and K

The shape of all graphs in Figure 3.7 is the same. One aspect is interest enough to explain. All graphs show a maximum load at a certain column length. This illustrates that a short column can resist less load than a longer column. This cannot be explained by normal forces. The explanation of the strange shape can be found in the bending moments. The bending moments depend on the rotation at the end of the beam and the deflection of the column. A short column cannot deflect easily $\left(\varphi = \frac{ML_{cln}}{3EI_{cln}} \rightarrow M = \frac{3\varphi EI_{cln}}{L_{cln}} \right)$. If the column length deceases, the bending moment increases. The stress in the column due to the bending moments increases. This results in a lower ultimate load.

Chapter 4 Braced portal frame

This Chapter is about a braced portal frame. The unbraced portal frame has been discussed in Chapter three. The main difference between the braced portal frame and the unbraced portal frame is the horizontal displacement of the beam. The horizontal displacement is limited in a braced situation.

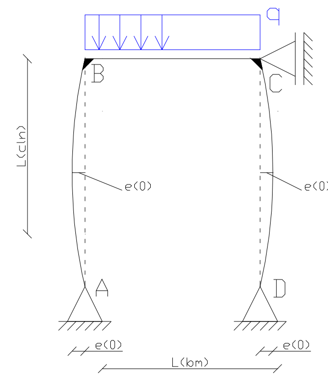

Figure 4.1: Structure

The construction imperfections have been discussed in Chapter three. In an unbraced structure, the construction imperfections are very important for the stability calculations. In a braced situation the horizontal deflection is limited. The influence of the production imperfections is very small. Te production imperfections can be neglected. The initial deflection of a braced portal frame is the same as the initial deflection of a single column. The column of the portal frame is curved (Fig. 4.1). As same as the unbraced portal frame (Chapter three) the braced portal frame is supported by hinges.

The columns and the beam are fixed together. The rotation at the end of the column is equal to the rotation at the end of the beam. A rotation of the beam results in a deflection of the column and a rotation of the column results in a deflection of the beam. The portal frame is loaded by a uniformly distributed load. Because of the load, the beam deflects, the end of the beam rotates and the column deflects.

The presence of the beam limits the deflection of the column in a second order calculation. The deflection of the first order calculation of the column of a braced portal frame is larger than the deflection of the first order calculation of a single column. This relation can be changed in the second order calculation.

4.1 Failure of the structure

It is assumed that the columns are critical. The beam will not fail. This assumption must be checked afterwards. The columns are loaded by normal forces and bending moments. If the dead loads of the columns are neglected, the normal forces in the columns are constant. The bending moments are variable over the length of the column. These moments depend on the reaction forces and on the deflection of the column. The distribution of the bending moments is not predictable at the start of the calculation. There are a few moment distributions possible (Fig. 4.2). A column can fail on many locations.

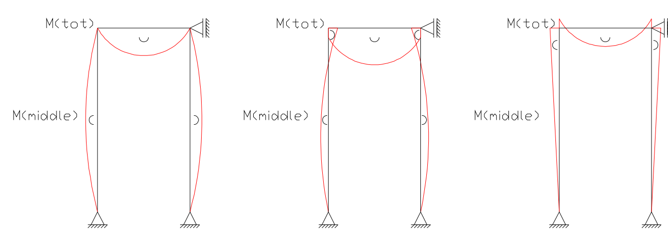

Figure 4.2: Moment distribution

The boundary conditions for both ends of the column are not equal. The support is free of bending moments and can rotate easily. The other end of the column is connected to the beam and has a rotation limitation. This end can resist some bending moments. Due to these different ends, the maximum deflection is not exactly in the middle of the column. The differences between the real maximum deflection and the deflection in the middle of the column are very small. It is assumed that the maximum deflection is in the middle of the column.

A non-slender column has a small deflection. The location of the maximum bending moment is at the end of the column. A slender column has a large deflection. The location of the maximum bending moment is (more or less) in the middle of the column. The relative slenderness depends on the section properties and on the length of both the column and the beam. The middle of the column and the end of the column are two logical failure locations. These two locations will be analyzed. The lowest load is the ultimate load of the structure.

4.2 Calculation according to the analysis of Appendices N and O

The portal frame is a two degrees statically undetermined structure. Because of symmetry, the horizontal support in point C can be taken zero. The other reaction forces can be calculated by equilibrium conditions and rotational equilibrium. The columns AB and CD are loaded equally. Both columns fail at the same load. In the analyses, the columns are critical. Failure of the beam must be checked afterwards.

The column of the portal frame can be schematized as a single column. The uniformly distributed load on the beam results in a formal force and a bending moment on the column and a rotation of the column. The beam limits the rotation of the column. This limitation can be schematized as a rotational spring.

For the calculation of the ultimate load a geometrical linear analysis and a geometrical non-linear analysis have been made. As same as the analyses of the unbraced portal frame, the results of the analyses will be limited by physical properties. The geometrical linear analysis can be found in Appendix M. The geometrical non-linear analysis can be found in Appendix N. In Appendix O the geometrical non-linear analysis has been extended by the influence of residual stress.

The geometrical linear analysis (based on equilibriums) results in a formula of the bending moments and in a formula of the maximum deflection. The results of the geometrical linear analysis together with the imperfection are used as initial position for the geometrical non-linear analysis.

The geometrical non-linear analysis is based on the equilibrium between the internal and the external bending moments. The internal moments are partial the bending of the column multiplied by the stiffness of the column and partial the bending of the beam multiplied by the stiffness of the beam. This last part is included in the rotational spring. The external moments are the total load multiplied by the total deflection and the bending moment at point C.

The geometrical non-linear analysis results in three sets of formulas to calculate the ultimate load. The first set can be used till the right flange starts to yield. The second set can be used till the right flange fully yields or till the left flange starts to yield. The third set can be used if both flanges partial yield. The different parts are equal to the different parts in the unbraced portal frame. The different parts are discussed in Section 3.4. Due to the different moment distributions, the third set of formulas is hardly used.

The following formulas can be used to calculate the additional deflections:

$$e_1 = \frac{q_1 L_{bm} L_{cln}{}^2 \left(q_1 L_{bm}{}^3 L_{cln}{}^2 + 64 e_0 \left(3L_{bm} EI_{cln,1} + 2L_{cln} EI_{bm} \right) + 16 L_{bm}{}^2 EI_{cln,1} \right)}{8\left[3\pi q_1 L_{bm} L_{cln}{}^3 EI_{bm} + \left(16\pi^2 EI_{cln,1} - 8q L_{bm} L_{cln}{}^2 \right)\left(3L_{bm} EI_{cln,1} + 2L_{cln} EI_{bm} \right) \right]}$$

$$e_2 = \frac{q_2 L_{bm} L_{cln}{}^2 \left(\begin{array}{l} \left(\left(q_1 + q_2 \right) L_{bm} L_{cln}{}^2 + 16 EI_{cln,2} \right)\left(3L_{bm} EI_{cln,1} + 2L_{cln} EI_{bm} \right)\left(L_{bm}{}^2 EI_{cln,2} + 6 L_{cln} z_2 EI_{bm} \right) \\ + \left(3L_{bm} EI_{cln,2} + 2L_{cln} EI_{bm} \right) \left(\begin{array}{l} 4\left(q_1 + q_2 \right) L_{bm} L_{cln}{}^2 z_2 \left(3L_{bm} EI_{cln,1} + 2L_{cln} EI_{bm} \right) \\ + L_{cln} EI_{cln,2} \left(q_1 L_{bm}{}^3 L_{cln} - 24\pi e_1 EI_{bm} \right) \\ + 64 EI_{cln,2} \left(3L_{bm} EI_{cln,1} + 2L_{cln} EI_{bm} \right)\left(e_0 + e_1 \right) \end{array} \right) \end{array} \right)}{8 EI_{cln,2} \left(3L_{bm} EI_{cln,1} + 2L_{cln} EI_{bm} \right) \left(\begin{array}{l} 3\pi \left(q_1 + q_2 \right) L_{bm} L_{cln}{}^3 EI_{bm} \\ + 8\left(2\pi^2 EI_{cln,2} - \left(q_1 + q_2 \right) L_{bm} L_{cln}{}^2 \right)\left(3L_{bm} EI_{cln,2} + 2L_{cln} EI_{bm} \right) \end{array} \right)}$$

$$e_3 = \frac{\begin{array}{l} q_3 L_{bm}{}^3 L_{cln}{}^2 EI_{cln,2} \left(\left(q_1 + q_2 + q_3 \right) L_{bm} L_{cln}{}^2 + 16 EI_{cln,3} \right)\left(3L_{bm} EI_{cln,1} + 2L_{cln} EI_{bm} \right)\left(3L_{bm} EI_{cln,2} + 2L_{cln} EI_{bm} \right) \\ + \left(\begin{array}{l} q_3 L_{bm} L_{cln}{}^3 \left(\begin{array}{l} q_2 L_{bm} L_{cln} \left(L_{bm}{}^2 EI_{cln,2} + 6 L_{cln} z_2 EI_{bm} \right) \\ - 24\pi e_2 EI_{bm} EI_{cln,2} \end{array} \right)\left(3L_{bm} EI_{cln,1} + 2L_{cln} EI_{bm} \right) \\ + q_3 L_{bm} L_{cln}{}^2 \left(3L_{bm} EI_{cln,2} + 2L_{cln} EI_{bm} \right) \\ \left(\begin{array}{l} L_{cln} EI_{cln,2} \left(q_1 L_{bm}{}^3 L_{cln} - 24\pi e_1 EI_{bm} \right) \\ + \left(64 EI_{cln,2} \left(e_0 + e_1 + e_2 \right) + 4 q_2 L_{bm} L_{cln}{}^2 z_2 \right)\left(3L_{bm} EI_{cln,1} + 2L_{cln} EI_{bm} \right) \end{array} \right) \end{array} \right)\left(3L_{bm} EI_{cln,3} + 2L_{cln} EI_{bm} \right) \end{array}}{\begin{array}{c} 8 EI_{cln,2} \left(3L_{bm} EI_{cln,1} + 2L_{cln} EI_{bm} \right)\left(3L_{bm} EI_{cln,2} + 2L_{cln} EI_{bm} \right) \\ \left(\begin{array}{l} 3\pi \left(q_1 + q_2 + q_3 \right) L_{bm} L_{cln}{}^3 EI_{bm} \\ + 8\left(2\pi^2 EI_{cln,3} - \left(q_1 + q_2 + q_3 \right) L_{bm} L_{cln}{}^2 \right)\left(3L_{bm} EI_{cln,3} + 2L_{cln} EI_{bm} \right) \end{array} \right) \end{array}}$$

The formulas for the total deflections are:

$$y_{total,1} = \frac{q_1 L_{bm}{}^3 L_{cln}{}^2}{64\left(3L_{bm} EI_{cln,1} + 2L_{cln} EI_{bm} \right)} + e_0 - \frac{\varphi_{extra,1,x=0} L_{cln}{}^2 EI_{bm}}{8 L_{bm} EI_{cln}} + e_1$$

$$y_{total,2}=\frac{q_1L_{bm}{}^3L_{cln}{}^2}{64\left(3L_{bm}EI_{cln,1}+2L_{cln}EI_{bm}\right)}+\frac{q_2L_{bm}L_{cln}{}^2\left(L_{bm}{}^2EI_{cln,2}+6L_{cln}z_2EI_{bm}\right)}{64EI_{cln,2}\left(3L_{bm}EI_{cln,2}+2L_{cln}EI_{bm}\right)}+e_0-\frac{\varphi_{extra,1,x=0}L_{cln}{}^2EI_{bm}}{8L_{bm}EI_{cln}}$$

$$-\frac{\varphi_{extra,2,x=0}L_{cln}{}^2EI_{bm}}{8L_{bm}EI_{cln,2}}+e_1+e_2+\frac{q_2L_{bm}L_{cln}{}^2z_2}{16EI_{cln,2}}$$

$$y_{total,3}=\frac{q_1L_{bm}{}^3L_{cln}{}^2}{64\left(3L_{bm}EI_{cln,1}+2L_{cln}EI_{bm}\right)}+\frac{q_2L_{bm}L_{cln}{}^2\left(L_{bm}{}^2EI_{cln,2}+6L_{cln}z_2EI_{bm}\right)}{64EI_{cln,2}\left(3L_{bm}EI_{cln,2}+2L_{cln}EI_{bm}\right)}+\frac{q_3L_{bm}{}^3L_{cln}{}^2}{64\left(3L_{bm}EI_{cln,3}+2L_{cln}EI_{bm}\right)}+e_0$$

$$-\frac{\varphi_{extra,1,x=0}L_{cln}{}^2EI_{bm}}{8L_{bm}EI_{cln}}-\frac{\varphi_{extra,2,x=0}L_{cln}{}^2EI_{bm}}{8L_{bm}EI_{cln,2}}-\frac{\varphi_{extra,3,x=0}L_{cln}{}^2EI_{bm}}{8L_{bm}EI_{cln,3}}+e_1+e_2+e_3+\frac{q_2L_{bm}L_{cln}{}^2z_2}{16EI_{cln,2}}$$

The additional rotation:

$$\varphi_{extra,1,x=0}=\frac{3\pi L_{bm}e_1EI_{cln,1}}{L_{cln}\left(3L_{bm}EI_{cln,1}+2L_{cln}EI_{bm}\right)}$$

$$\varphi_{extra,2,x=0}=\frac{3\pi L_{bm}e_2EI_{cln,2}}{L_{cln}\left(3L_{bm}EI_{cln,2}+2L_{cln}EI_{bm}\right)}$$

$$\varphi_{extra,3,x=0}=\frac{3\pi L_{bm}e_3EI_{cln,3}}{L_{cln}\left(3L_{bm}EI_{cln,3}+2L_{cln}EI_{bm}\right)}$$

The horizontal reaction forces:

$$F_1=\frac{q_1L_{bm}{}^3EI_{cln,1}}{4L_{cln}\left(3L_{bm}EI_{cln,1}+2L_{cln}EI_{bm}\right)}$$

$$\Delta F_1=\frac{3\varphi_{extra,1,x=0}EI_{cln,1}}{L_{cln}{}^2}$$

$$F_2=\frac{q_2L_{bm}\left(L_{bm}{}^2EI_{cln,2}+6L_{cln}z_2EI_{bm}\right)}{4L_{cln}\left(3L_{bm}EI_{cln,2}+2L_{cln}EI_{bm}\right)}$$

$$\Delta F_2=\frac{3\varphi_{extra,2,x=0}EI_{cln,2}}{L_{cln}{}^2}$$

$$F_3=\frac{q_3L_{bm}{}^3EI_{cln,3}}{4L_{cln}\left(3L_{bm}EI_{cln,3}+2L_{cln}EI_{bm}\right)}$$

$$\Delta F_3=\frac{3\varphi_{extra,3,x=0}EI_{cln,3}}{L_{cln}{}^2}$$

The vertical reaction force:

$$N_1=0.5q_1L_{bm}$$

$$N_2=0.5q_2L_{bm}$$

$$N_3 = 0.5 q_3 L_{bm}$$

The additional bending moments can be calculated by the follow formulas.

$$M_{top,1} = (F_1 - \Delta F_1) L_{cln}$$
$$M_{middle,1} = 0.5(F_1 - \Delta F_1) L_{cln} + 0.5 q_1 L_{bm} e_{total,1}$$

$$M_{top,2} = (F_2 - \Delta F_2) L_{cln}$$
$$M_{middle,2} = 0.5(F_2 - \Delta F_2) L_{cln} + 0.5 q_1 L_{bm} (e_{total,2} - e_{total,1}) + 0.5 q_2 L_{bm} e_{total,2}$$

$$M_{top,3} = (F_3 - \Delta F_3) L_{cln}$$
$$M_{middle,3} = 0.5(F_3 - \Delta F_3) L_{cln} + 0.5(q_1 + q_2) L_{bm} (e_{total,3} - e_{total,2}) + 0.5 q_3 L_{bm} e_{total,3}$$

A calculations example has been made in Appendix P.

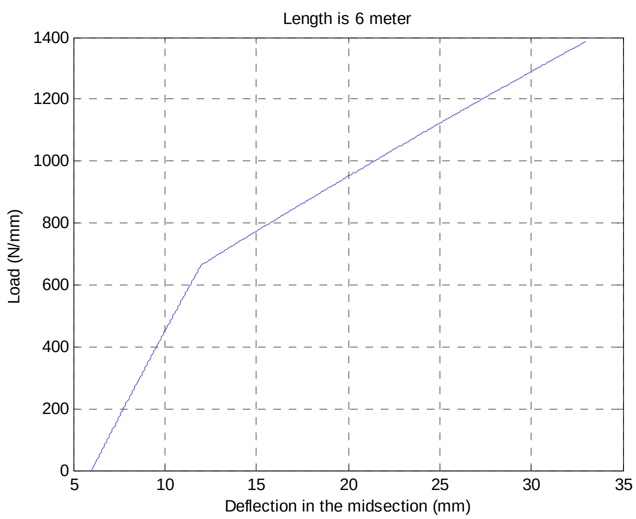

Calculation braced portal frame

Column: Length: 6 m
HE 360A

Beam: Length: 5 m
HE 900A

S355

e0 = 6 mm

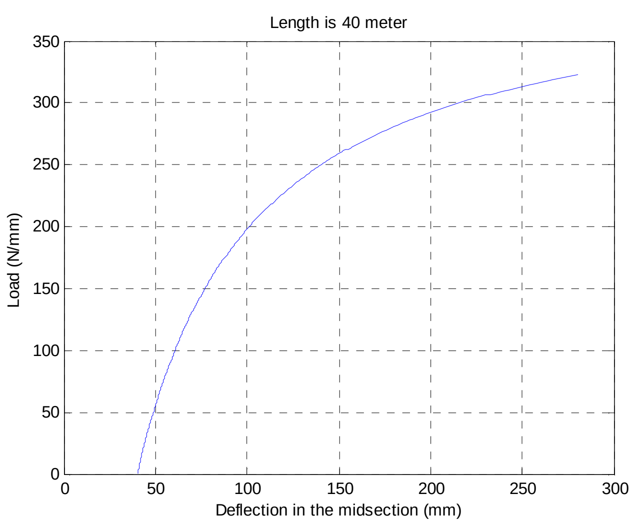

Calculation braced portal frame

Column: Length: 40 m
HE 360A

Beam: Length: 5 m
HE 900A

S355

e0 = 40 mm

Figure 4.3: Load-deflection graphics

Figure 4.3 shows two load-deflection graphs for a braced portal frame. For the top graph the first and the second set of formulas have been used. For the lowest graph only the first set is used. After partial yield, the stiffness was reduced too much. Another difference between the graphs is the location of the largest bending moment. In the top graph, the maximum bending moment is at the end of the column. The maximum bending moment in the lowest graph is located in the middle of the column.

4.3 Calculation according to the Dutch code

According to the NEN 6771 the calculations of a braced portal frame is the same as for an unbraced portal frame (Section 3.5). The main difference between the braced and the unbraced calculation method is the buckling length. The buckling length of a braced portal frame is maximum the column length. The buckling length of an unbraced portal frame is at least twice the column length. Other differences are the input parameters (See App. G for more details).

The uniformly distributed load on the portal frame must be transformed to a bending moment and a normal force. This can be done by a linear calculation. (See App. P.3 for a calculation example according the Dutch code.) The ultimate load can be calculated by the following formula:

$$\frac{N_{c;s;d}}{N_{c;u;d}} + \frac{n_y}{n_y - 1}\frac{M_{y;equ;s;d} + N_{c;s;d}e_y^*}{M_{y;u;d}} \leq 1.0 \qquad \text{(art. 12.3.1.2.1)}$$

In this formula is:

$N_{c;s;d}$, $M_{y;equ;s;d}$	The loads on the column
$N_{c;u;d}$	Plastic normal force
n_y	Relation between the Euler buckling load and the load on the structure (Note: for the Euler buckling load, the buckling length must be taken)
$M_{y;u;d}$	Plastic bending moment
e_y^*	Imperfection parameter

e_y^* must be calculated by the following formula:

$$e_y^* = \alpha_k\left(\lambda_{y;rel} - \lambda_0\right)\frac{M_{y;u;d}}{N_{c;u;d}}$$

4.4 Calculation according to Matrix Frame

Matrix Frame has been used to calculate the ultimate load of a braced portal frame. The beam has been made strong enough to be sure that the columns are critical. The columns are split is small elements. Different horizontal displacements of the joints simulate the initial deflection. This schematization of the imperfections is as same as in the calculation of the single column (Section 2.9 or App. F). Imperfections of the beam are not taken into account.

Two different calculations are made. One calculation with residual stresses and one calculation without residual stresses. The residual stress is inserted by using two calculations. The section properties of all construction elements are bisected. In the first calculation of the ultimate load, all sections have steel grade S235. In the second calculation of the ultimate load, all sections have steel grade S460. The summation of these calculations is the total ultimate load. The amount of residual stress in the Matrix Frame calculation does not correspond with the amount of residual stress in the analysis. The amount of residual stress must be larger. This cannot be done because of the input limitations of Matrix Frame.

Figure 4.4 shows two load-deflection graphs. The red curve is the calculation without residual stress. The blue curve is the calculation with residual stress.

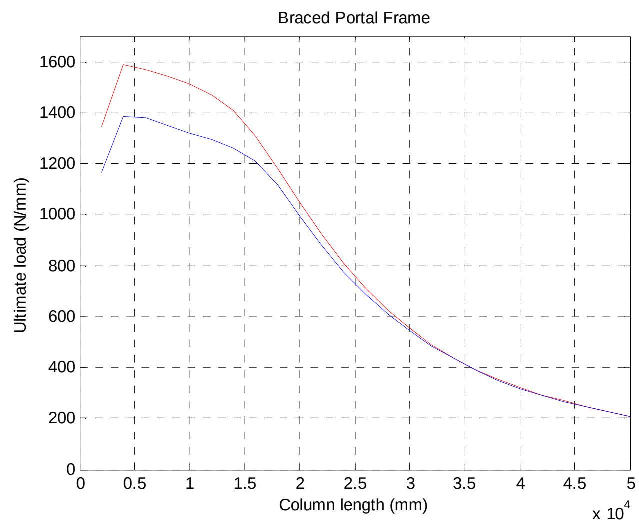

Figure 4.4: Load-deflection graphics

The curve with residual stress is lower than the curve without residual stress. The difference between the calculation with and without residual stresses decreases from fifteen percent for non-slender structures till zero for slender structures. The curve for the ultimate load calculation including residual stress will be used as comparison for calculation methods.

The calculation file of Matrix Frame can be found in Appendix P.4.

4.5 Conclusions

Chapter four was related to a braced portal frame. The ultimate load has been calculated by three calculation methods. The results of the calculations are expressed in a load-deflection graph (Fig. 4.5).

An analysis is made to find three sets of formulas for the additional deflection. These sets correspond to different yield phases of the structure. These formulas can be used to calculate the ultimate load. This calculation method is the blue curve in Figure 4.5.

To calculate the ultimate load according to the Dutch code (red curve) a linear analysis must be made. The uniformly distributed load must be transformed to normal forces and bending moments. These values can be used as input for the unity checks.

The Matrix Frame calculation is divided in two parts. Both parts have a different yield stress. Both parts together illustrate the residual stress. The real amount of stress cannot be schematized in Matrix Frame. The result of this calculation method is the green curve in Figure 4.5.

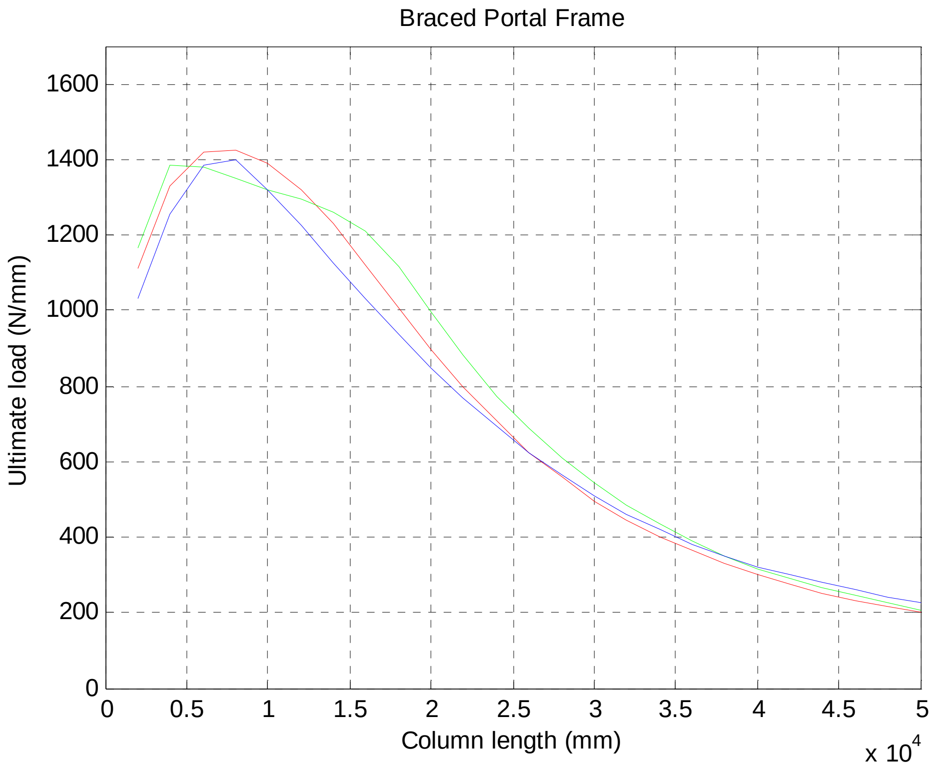

Calculation braced portal frame

Column:
Length: variable
HE 360A
Beam: Length: 5 m
HE 900A

S355

Figure 4.5: Ultimate load graphs

- The red curve is the load according to the Dutch code
- The green curve in the load according to the Matrix Frame
- The blue curve is the load according to the analysis in Appendices N and O

The graphs of figure 4.5 shows some points of attention.

The first point of attention is the curve according to the Dutch code. The calculation according to the Dutch code does not always results in the lowest ultimate load. For the lengths between five and thirteen meters (for this calculation example) the results of the code calculation are larger than the results of the Matrix Frame calculation. In the Matrix Frame calculation the amount of residual stress is lower than it should be. The calculated ultimate load is the summation of two calculations. Due to the geometrical and physical deflections, the calculated ultimate load is a bit larger than the real ultimate load. This should contain that Matrix Frame calculation is an upper limit for the real ultimate load.

The same problem has been seen in the buckling calculations of the single column. Figure 2.15 (repeated in Figure 4.6) shows stability curves for several calculation methods. According to Matrix Frame (green curve), the structure cannot reach

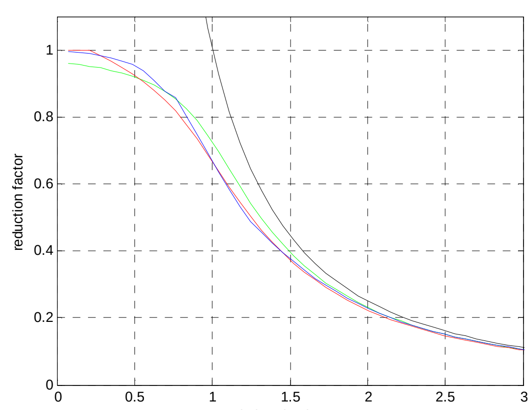

Figure 4.6: Stability curve for several calculations methods

the plastic yield load. For non-slender structures, the results of the buckling calculations according to Matrix Frame are smaller than the results of the code calculations (red curve).

The cut down top of the graph (Fig. 4.5) can be explained by not reaching the plastic yield load in the Matrix Frame calculation

The second point of attention is the comparison between the code calculations and the analysis calculations (Fig. 4.5). The differences are very small. For slender structures the analysis calculation results in a higher ultimate load and for non-slender structures the analysis calculation results in a smaller ultimate load. The analysis calculation can be used to calculate the ultimate load for a braced portal frame.

Chapter 5 Extended Frame

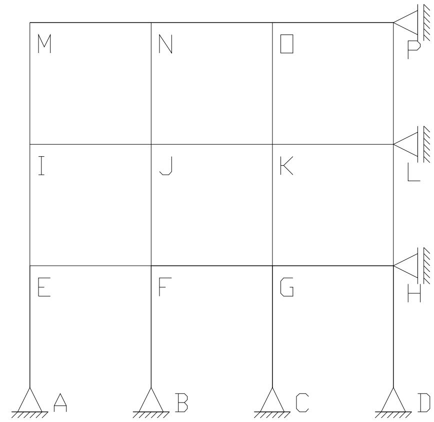

Figure 5.1: Structure

The last analyzed structure of this study is a braced extended frame. The extended frame has three floors and three bays. The frame is vertically supported on four hinges (Fig. 5.1).

All construction elements are fixed together. The structure will be loaded by some point loads and some uniformly distributed loads. Due to these loads, the beams and the columns deflect.

If the columns deflect, the connected ends rotate and the connected construction elements deform. The whole structure will resist if the columns deflects due to second order effects.

5.1 *Initial deflections*

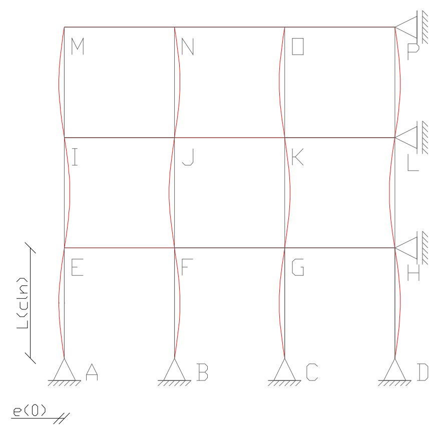

Figure 5.2: Imperfections

The frame exists in many columns and many beams. It is assumed that the columns are critical. Failure mechanisms of the beams are not taken into account. The initial deflections of the beam have no effect on the stress distribution of the columns. The initial deflections of the beams are neglected.

The extended frame is braced. In other words: the ends of the column will not displace in lateral direction. The initial deflection of the columns in this frame is taken equally to the initial deflection of a single column (Chapter one). The initial deflection of the column is a half sine shape. The maximum deflection is one over thousand times the column length (NEN 6771 art. 10.2.5..1.3). See Figure 5.2 for the starting deflections.

The direction of the initial deflections is taken in the most unfavourable direction. The most unfavourable direction is the direction in which the column deflects due to the load on the structure. The loads on the structure will be discussed in Section 5.2.

5.2 *Loads*

The loads on the structure are based on the requirements of the Dutch code. The NEN 6702 is about loading rules and safety rules. This volume of the Dutch code is used to calculate the ultimate load. The NEN 6702 describes three types of loads: permanent loads, variable loads and special loads. The different loads are worked out in Appendix Q.

The permanent load of the column is the dead load of the column only. The permanent load of the beam is partial the dead load of the beam, partial the dead load of a floor and partial the dead load of a partition wall. Wind load have a positive influence on the stability of the structure. The influence of wind load is neglected. Special loads are not taken into account in this study. The permanent loads and the variable loads are uniformly distributed loads on the floors. Due to symmetry, the permanent loads can be schematized as point loads. Some floors are loaded by a heavy vertical variable load. The variable loads are not located on every floor. It is not allowed to schematize these loads as point loads.

The extended frame is heaviest loaded if all floors are loaded. The probability that all floors are maximum loaded is very small. According to the Dutch code (NEN 6702) it is not necessary to calculate with this extremely load-situation. It is allowed to keep some floors free of variable loads. For the second order analysis the largest deflection is most interesting. For the highest deflections, the frame is loaded symmetrically. Two load combinations are calculated (see Fig. 5.3 and Fig. 5.4 for the different load combinations).

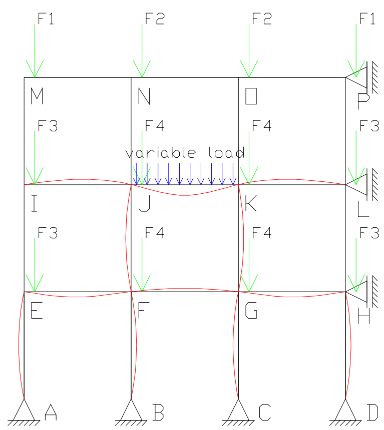

Figure 5.3:
Load combination

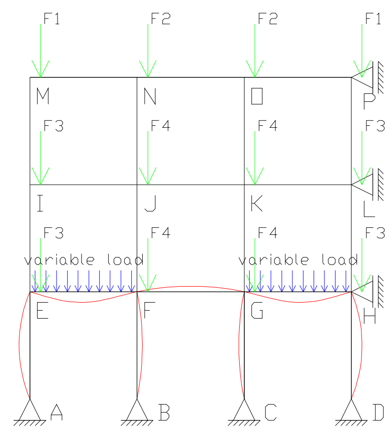

Figure 5.4:
Load combination

In the first load combination only one floor is loaded by a variable load. Due to this load, the columns are loaded by normal forces and by bending moments. The maximum normal force can be found in column BF and in column CG. The difference between the normal force in column BF and the normal force in column FJ is the required load F_4. The required loads are very small compare with the variable loads. There is only a small difference between the normal forces.

The bending moments in column FJ and the bending moments in column GK are much larger than the bending moments in other columns of the structure. Taken the combination between the bending moments and the normal forces, column FJ and column GK are loaded heaviest. The analysis and the calculation are about failure of column FJ.

In the second load combination two floors are loaded by a variable load. Again there is a difference between the largest normal forces and the largest bending moments. Column BF and column CG are loaded by the largest normal forces. Column AE and column DH are loaded by the largest bending moments. Because of time limit and complexity the second load combination has not been analyzed. The different load cases are compared together using of a computer made finite element analysis (App. U.4).

For only the first load combination, an analytical solution is found. This Chapter is mainly concentrated on the first load combination.

5.3 Elongations

The most important issue of the non-linear analysis is the deflection. The moment distribution in the frame is related to the deflections of the frame. Instead of other structures, the columns of the extended frame are not loaded equally. The columns in the middle of the structure are heavy loaded while the loads on the columns at the sides of the structure are very small. This results in elongation differences.

The study is based on a strong beam/weak column analysis. A weak column contains a small moment of inertia and a small cross-section. A small cross-section results in large elongations $\left(\delta = \frac{FL_{cln}}{EA_{cln}} \right)$.

Due to the uniformly distributed load, all beams contain bending moments. These bending moments result in a rotation at the end of the beam. Elongation differences result in a rotation of the beam too. The following formulas can be used to calculate the rotations.

$$\varphi_1 = \frac{ML_{bm}}{3EI_{bm}}$$

$$\varphi_2 = \frac{FL_{cln}}{L_{bm}EA_{cln}}$$

The rotation due to the bending moments depends on the section properties of the beam. The rotation due to the elongation differences depends on the section properties of the column. A combination of a slender column and a non-slender beam results is a major influence of the elongation differences. For slender columns, the elongation differences must be taken into account.

Figure 5.5 shows two structures. In both structures the bending moment distribution is displayed. In the left structure, the elongation is neglected. In the right structure, the elongation is taken into account. The differences between these structures are the numerical value of the bending moments. In the structure of figure 5.5, the bending moments in the column increase with 35% if elongation is taken into account. This difference cannot be neglected.

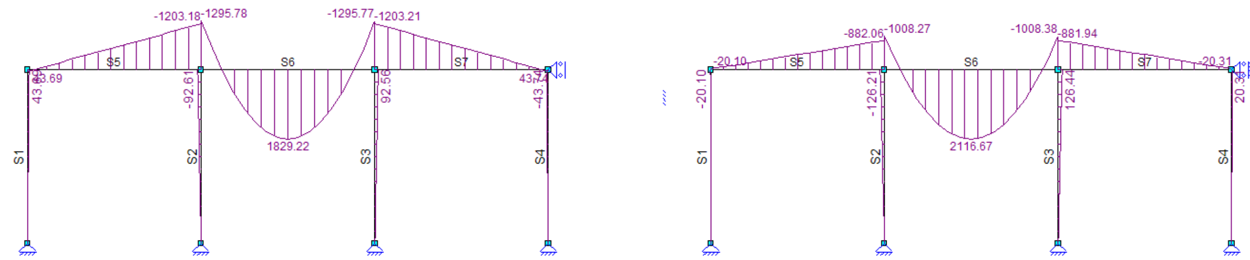

Without elongations

With elongations

Figure 5.5: Bending moments

Figure 5.6 contains two graphs. Both graphs contain the ultimate load for the extended frame, calculated by the analysis of Appendices S and T (Section 5.4). In the blue curve, the elongation differences are not taken into account. The elongation differences are taken into account at the green curve. Both curves have the same shape (will be discussed in Section 5.7). The numerical differences between the curves are about 15%. The elongation differences are taken into account at the ultimate load calculation according to the analysis.

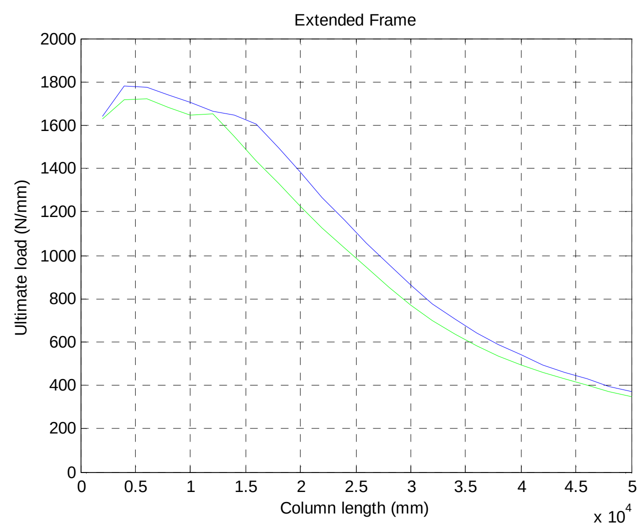

Figure 5.6: Ultimate load graphics

5.4 Calculation according to the analysis of Appendices S and T

For the calculation of the ultimate load, a geometrical linear (App. R) and a geometrical non-linear analysis (App. S and App. T) are made. As same as in the braced portal frame (Chapter four), the results of the linear analysis is the input for the non-linear analysis. Physical properties are used as limitations for the results of the ultimate load calculation.

Due to the load, column FJ and column GK are heaviest loaded. It is assumed that only these columns yield and fail. Due to the symmetry of the structure and the symmetry of the load, column FJ and column GK are loaded equally. Column FJ and column GK yield at the same moment.

All elements of the structure are connected together. If one element of the structure is loaded, all elements deflect. The load will be carried by the whole structure. The stiffness of all structure elements has effect on the deflection of the loaded element. It is nearly impossible to take the deflection of all elements into account in a manual analysis. Some virtual hinges are used to make the analysis manageable. The loaded element is beam JK.

The column JN and FJ and beam IJ have a major influence on the deflection of beam JK. The bending moments on both sides of these construction elements are taken into account. For simplicity the deflections of other construction elements are neglected. In other words: a virtual hinge is taken in the points E, H, M and P.

As same as in the analysis of the braced portal frame, the column has been schematized as a single column. The initial deflection for the geometrical non-linear analysis is partial the starting deflection (imperfections) and partial geometrical linear deflection (due to the uniformly distributed load). The influence of all construction elements has been schematized as a rotational spring on both sides of the column. The stiffness of these springs depends on the different construction elements. Because of safety only one fourth of the stiffness of the structure is taken into account.

The non-linear analysis of the frame is based on the equilibrium between the internal bending moments and the external moments in column FJ. The internal moments are partial the bending of the column multiplied by the stiffness of the column and partial the bending moments of the rotational spring. The external bending moments are partial the normal force multiplied by the total deflection and partial the bending total bending moments at the ends of the column.

The required loads are much smaller than the ultimate loads. The influences of the required loads on the additional deflection are very small. The analysis becomes much more complex if the required loads are taken into account. At the analysis of the residual stress the formulas become unmanageable if the required loads are taken into account. For simplicity and because of the small influence the required loads are neglected in the analysis. The required loads are taken into account at the calculation of the stresses.

The residual stress distribution has been discussed in Chapter one. The same residual stress distribution will be used in the analysis of the extended frame (Fig. 5.7 as reminder). Due to the presence of residual stress, a loaded section will partial yield before the structure fails. The stiffness decreases if the section partial yields. A reduced stiffness results in larger deflections.

The spring stiffness does not depend on the stiffness of yielded columns (FJ and GK), but on the stiffness of the other construction elements. The stiffness of these elements remains constant. The stiffness of the rotation spring remains constant too.

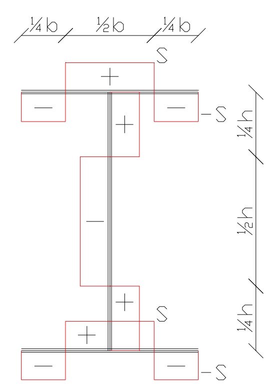

Figure 5.7: Residual stress distribution

In Appendix S a geometrical non-linear analysis of an extended frame has been made. In Appendix T the geometrical non-linear analysis is extended by the influence of residual stress. The physical properties limit the result of the geometrical non-linear calculation. The analysis of Appendix T results in much more complex formulas than the analysis in Appendix S. Totally three sets of formulas are found.

The following formulas can be used to calculate the additional deflection:

$$e_1=\frac{\begin{array}{l}qL_{bm}L_{cln}^{\;2}\left(11L_{bm}EI_{cln}+5L_{cln}EI_{bm}\right)\left(24e_0EI_{cln}+L_{cln}^{\;2}\left(M_{J,bottom}-M_{F,top}\right)\right)\\ +24\left(M_{J,bottom}+M_{F,top}\right)L_{cln}^{\;2}EI_{cln}\left(11L_{bm}EI_{cln}+5L_{cln}EI_{bm}\right)\end{array}}{6EI_{cln}\begin{pmatrix}8\pi^2EI_{cln}\left(11L_{bm}EI_{cln}+5L_{cln}EI_{bm}\right)\\ +qL_{bm}L_{cln}^{\;2}\left(\left(3\pi-44\right)L_{bm}EI_{cln}+\left(5\pi-20\right)L_{cln}EI_{bm}\right)\end{pmatrix}}$$

$$e_2=\frac{\begin{pmatrix}2L_{bm}L_{cln}^{\;4}\begin{pmatrix}\left(q_1+q_2\right)\left(M_{J,bottom,2}-M_{F,top,2}\right)EI_{cln,1}\\ +q_2\left(M_{J,bottom,1}-M_{F,top,1}\right)EI_{cln,2}\end{pmatrix}\left(11L_{bm}EI_{cln,1}+5L_{cln}EI_{bm}\right)\begin{pmatrix}8L_{bm}EI_{cln,2}+3L_{bm}EI_{cln,1}\\ +5L_{cln}EI_{bm}\end{pmatrix}\\ +24q_2\left(q_1+q_2\right)L_{bm}^{\;3}L_{cln}^{\;4}z_2EI_{cln,1}EI_{cln,2}\left(11L_{bm}EI_{cln,1}+5L_{cln}EI_{bm}\right)\\ +12q_2L_{bm}L_{cln}^{\;2}EI_{cln,1}EI_{cln,2}\left(8L_{bm}EI_{cln,2}+3L_{bm}EI_{cln,1}+5L_{cln}EI_{bm}\right)\begin{pmatrix}4e_0\left(11L_{bm}EI_{cln,1}+5L_{cln}EI_{bm}\right)\\ +e_1\begin{pmatrix}\left(44-3\pi\right)L_{bm}EI_{cln,1}\\ +\left(20-5\pi\right)L_{cln}EI_{bm}\end{pmatrix}\end{pmatrix}\\ +48\left(M_{J,bottom,2}+M_{F,top,2}\right)L_{cln}^{\;2}EI_{cln,1}EI_{cln,2}\left(11L_{bm}EI_{cln,1}+5L_{cln}EI_{bm}\right)\left(8L_{bm}EI_{cln,2}+3L_{bm}EI_{cln,1}+5L_{cln}EI_{bm}\right)\end{pmatrix}}{12EI_{cln,1}EI_{cln,2}\left(11L_{bm}EI_{cln,1}+5L_{cln}EI_{bm}\right)\begin{pmatrix}4\left(2\pi^2EI_{cln,2}-\left(q_1+q_2\right)L_{bm}L_{cln}^{\;2}\right)\begin{pmatrix}8L_{bm}EI_{cln,2}+3L_{bm}EI_{cln,1}\\ +5L_{cln}EI_{bm}\end{pmatrix}\\ +\pi\left(q_1+q_2\right)L_{bm}L_{cln}^{\;2}\left(3L_{bm}EI_{cln,1}+5L_{cln}EI_{bm}\right)\end{pmatrix}}$$

$$e_3=\frac{\begin{bmatrix}2L_{bm}L_{cln}^{\;4}\begin{pmatrix}\left(q_1+q_2+q_3\right)\left(M_{J,bottom,3}-M_{F,top,3}\right)EI_{cln,1}EI_{cln,2}\\ +q_3\left(M_{J,bottom,1}-M_{F,top,1}\right)EI_{cln,2}EI_{cln,3}\\ +q_3\left(M_{J,bottom,2}-M_{F,top,2}\right)EI_{cln,1}EI_{cln,3}\end{pmatrix}\begin{pmatrix}11L_{bm}EI_{cln,1}\\ +5L_{cln}EI_{bm}\end{pmatrix}\begin{pmatrix}8L_{bm}EI_{cln,2}+3L_{bm}EI_{cln,1}\\ +5L_{cln}EI_{bm}\end{pmatrix}\begin{pmatrix}8L_{bm}EI_{cln,3}+3L_{bm}EI_{cln,1}\\ +5L_{cln}EI_{bm}\end{pmatrix}\\ +3q_3L_{bm}L_{cln}^{\;2}EI_{cln,1}EI_{cln,3}\begin{pmatrix}4EI_{cln,2}\begin{pmatrix}4\left(e_0+e_1+e_2\right)\left(11L_{bm}EI_{cln,1}+5L_{cln}EI_{bm}\right)\\ -\pi e_1\left(3L_{bm}EI_{cln,1}+5L_{cln}EI_{bm}\right)\end{pmatrix}\begin{pmatrix}8L_{bm}EI_{cln,2}+3L_{bm}EI_{cln,1}\\ +5L_{cln}EI_{bm}\end{pmatrix}\\ -\left(4\pi e_2EI_{cln,2}+q_2L_{bm}L_{cln}^{\;2}z_2\right)\left(11L_{bm}EI_{cln,1}+5L_{cln}EI_{bm}\right)\left(3L_{bm}EI_{cln,1}+5L_{cln}EI_{bm}\right)\end{pmatrix}\begin{pmatrix}8L_{bm}EI_{cln,3}+3L_{bm}EI_{cln,1}\\ +5L_{cln}EI_{bm}\end{pmatrix}\\ +48\left(M_{J,bottom,3}+M_{F,top,3}\right)L_{cln}^{\;2}EI_{cln,1}EI_{cln,2}EI_{cln,3}\begin{pmatrix}11L_{bm}EI_{cln,1}\\ +5L_{cln}EI_{bm}\end{pmatrix}\begin{pmatrix}8L_{bm}EI_{cln,2}+3L_{bm}EI_{cln,1}\\ +5L_{cln}EI_{bm}\end{pmatrix}\begin{pmatrix}8L_{bm}EI_{cln,3}+3L_{bm}EI_{cln,1}\\ +5L_{cln}EI_{bm}\end{pmatrix}\end{bmatrix}}{12EI_{cln,1}EI_{cln,2}EI_{cln,3}\begin{pmatrix}11L_{bm}EI_{cln,1}\\ +5L_{cln}EI_{bm}\end{pmatrix}\begin{pmatrix}8L_{bm}EI_{cln,2}+3L_{bm}EI_{cln,1}\\ +5L_{cln}EI_{bm}\end{pmatrix}\begin{pmatrix}\begin{pmatrix}8\pi^2EI_{cln,3}\\ -4\left(q_1+q_2+q_3\right)L_{bm}L_{cln}^{\;2}\end{pmatrix}\left(8L_{bm}EI_{cln,3}+3L_{bm}EI_{cln,1}+5L_{cln}EI_{bm}\right)\\ +\pi\left(q_1+q_2+q_3\right)L_{bm}L_{cln}^{\;2}\left(3L_{bm}EI_{cln,1}+5L_{cln}EI_{bm}\right)\end{pmatrix}}$$

To calculate the ultimate load, the formulas for the geometrical linear rotations, the geometrical linear bending moments and the additional rotation must be calculated too.

$$\varphi_J = \frac{qL_{bm}L_{cln}\begin{pmatrix} -1800L_{cln}{}^4\left(EI_{bm}\right)^4 - 8280L_{bm}L_{cln}{}^3\left(EI_{bm}\right)^3 EI_{cln} - 10980L_{bm}{}^2L_{cln}{}^2\left(EI_{bm}\right)^2\left(EI_{cln}\right)^2 \\ -4104L_{bm}{}^3L_{cln}EI_{bm}\left(EI_{cln}\right)^3 \\ -L_{bm}{}^3EA_{cln}\left(3L_{bm}EI_{cln}+2L_{cln}EI_{bm}\right)\left(4L_{bm}EI_{cln}+5L_{cln}EI_{bm}\right)\left(7L_{bm}EI_{cln}+5L_{cln}EI_{bm}\right) \end{pmatrix}}{24EA_{cln}\begin{pmatrix} 125L_{cln}{}^4\left(EI_{bm}\right)^4 + 445L_{bm}L_{cln}{}^3\left(EI_{bm}\right)^3 EI_{cln} + 1335L_{bm}{}^2L_{cln}{}^2\left(EI_{bm}\right)^2\left(EI_{cln}\right)^2 \\ +1287L_{bm}{}^3L_{cln}EI_{bm}\left(EI_{cln}\right)^3 + 270L_{bm}{}^4\left(EI_{cln}\right)^4 \end{pmatrix}}$$

$$M_{J,bottom} = \frac{EI_{cln}\left(3qL_{cln}{}^2EI_{bm} - 4\varphi_{J,bottom}EA_{cln}\left(6L_{bm}EI_{cln}+5L_{cln}EI_{bm}\right)\right)}{L_{cln}EA_{cln}\left(7L_{bm}EI_{cln}+5L_{cln}EI_{bm}\right)}$$

$$M_{F,top} = \frac{1.5qL_{cln}EI_{bm}}{L_{bm}EA_{cln}} + \left(\frac{3L_{bm}EI_{cln}+5L_{cln}EI_{bm}}{L_{bm}L_{cln}}\right)\varphi_F$$

$$\varphi_F = \frac{M_{J,bottom}L_{bm}L_{cln}EA_{cln} - 3qL_{cln}{}^2EI_{bm}}{2EA_{cln}\left(6L_{bm}EI_{cln}+5L_{cln}EI_{bm}\right)}$$

$$\varphi_{extra,2,x=0} = \frac{2L_{bm}\left(4\pi e_2 EI_{cln,2} + q_2L_{bm}L_{cln}{}^2z_2\right)}{L_{cln}\left(8L_{bm}EI_{cln,2}+3L_{bm}EI_{cln,1}+5L_{cln}EI_{bm}\right)}$$

$$\varphi_{extra,3,x=0} = \frac{8\pi L_{bm}e_3EI_{cln,3}}{L_{cln}\left(8L_{bm}EI_{cln,3}+3L_{bm}EI_{cln,1}+5L_{cln}EI_{bm}\right)}$$

A calculation example can be found in Appendix U.

5.5 Calculation according to the Dutch code

The ultimate load calculation for a braced extended frame is equal to the ultimate load calculation of the braced portal frame. This is clearly discussed in Section 4.3. The calculation of the ultimate load according to the Dutch code is based on the results of a geometrical linear analysis. Because of time limitation only a few calculations has been made. The results of the calculation can be found in Section 5.7.

5.6 Calculation according to Matrix Frame

As comparison, the ultimate load is calculated by Matrix Frame too. For a real comparison the initial deflection and the residual stress should be inserted manually in Matrix Frame. For the manual input of the imperfections every column must be split in four parts. Every joint must have a different horizontal displacement. The input of the Matrix Frame calculation is time consuming (every part must be changed if the length changes). The calculation time of Matrix Frame is time consuming too. It is chosen to calculate just a few lengths to make it possible to compare the results with the results of other calculation methods.

To take residual stress into account, two extra Matrix Frame calculations are needed. One with steel grade S235 and one with steel grade S460. The calculation method is the same as in other constructions and is clearly discussed in Section 2.9. Without the Matrix Frame calculation with residual stress, the comparison is not completed.

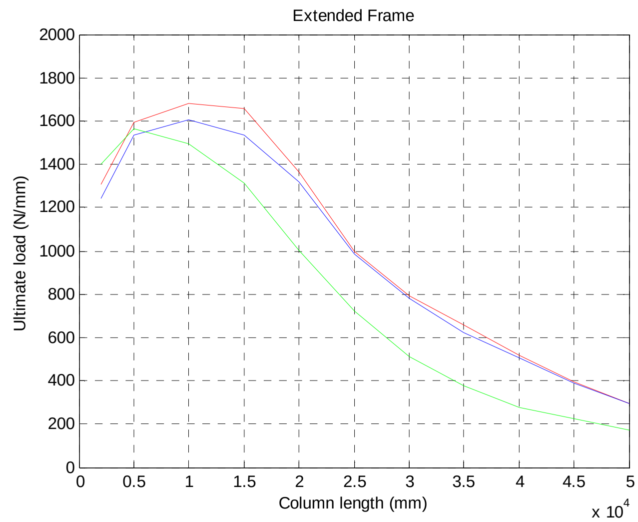

Figure 5.8: Ultimate load graphs

The amount of residual stress is (as same as in the portal frames) less than it should be. This is because of the input limitations of Matrix Frame. The results of both Matrix Frame calculations can be found in Figure 5.8. The red curve is the ultimate load without residual stress and the blue curve is the ultimate load with residual stress. As seen before in the calculation of a braced portal frame, the residual stress reduces the ultimate load.

The green curve is the calculation of another load combination (Fig. 5.4). The ultimate loads of this load combination are much lower (especially for slender structures). For the ultimate load calculation in this structure the wrong load combination is chosen. As academic model, this correct load combination is chosen.

For the chosen load combination a bending moment at both ends and an elongation difference must be taken into account. This is quite different as the analysis of a braced portal frame. The analysis of the second load combination can be made by the same way as did in Chapter four (braced portal frame). This analysis does not have an extra contribution to this study.

The blue curve will be used to compare the ultimate load with other calculation methods.

5.7 Conclusions

Three calculation methods are used to calculate the ultimate load of the extended frame. First a geometrical non-linear analysis is made. In this analysis residual stress is taken into account. The results of this calculation method are the blue curve in figure 5.9. Secondly the ultimate load is calculated according to the Dutch code (red curve). As third the ultimate load is calculated by Matrix Frame (green curve). Because of input limitations only a part of the residual stress is taken into account at the Matrix Frame calculations. The calculation according to the Dutch code and the calculations according to Matrix Frame are time consuming. Due to this, only a few calculations are made (every five meter instead of every two meter). This results in a less curved graph. The shape of the graphs is well visible.

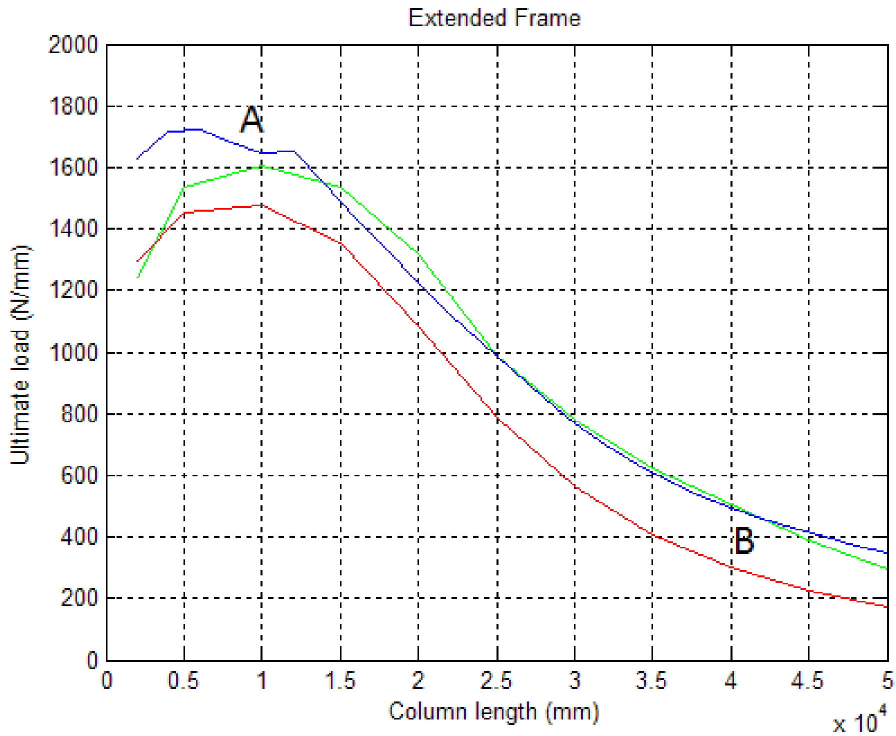

Calculation braced extended frame

Column:
Length: variable
HE 360A
Beam: Length: 5 m
HE 900A

S355

Figure 5.9: Ultimate load graphics

- The red curve is the load according to the Dutch code
- The green curve in the load according to the Matrix Frame
- The blue curve is the load according to the analysis in Appendices N and O

Two striking points of the graphs in Figure 5.9 will be discussed. These points are marked by the characters A and B.

Point A is a strange course of the graph. For a column length of ten meters, the ultimate load is smaller than for a column length of eight meters but also lower than for a column of twelve meters. This shape can be explained by looking at the internal stresses. The internal stresses for a column length of ten and twelve meters are given in Figure 5.10 and Figure 5.11.

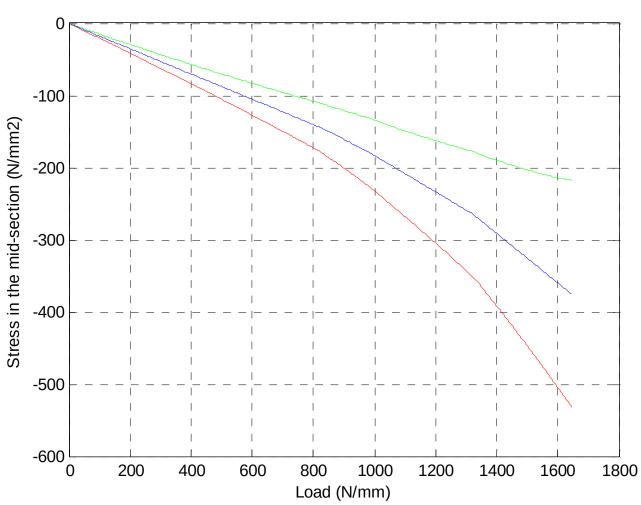

Calculation braced extended frame

Column:
Length: variable
HE 360A
Beam: Length: 10 m
HE 900A

S355

Figure 5.10: Internal stresses

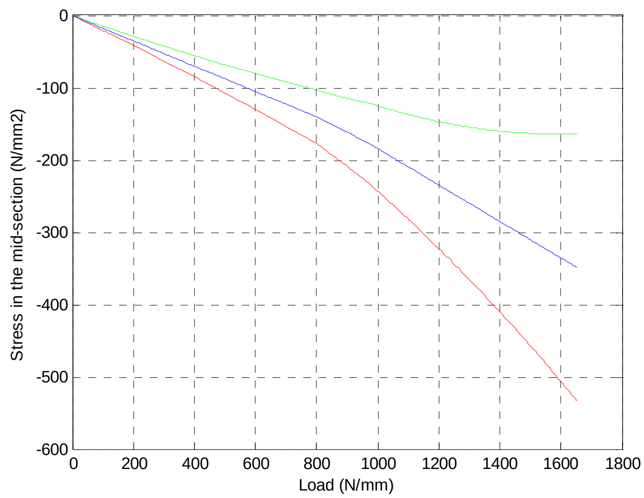

Calculation braced extended frame

Column:
Length: variable
HE 360A
Beam: Length: 12 m
HE 900A

S355

Figure 5.11: Internal stresses

- The red curve corresponds with the stress in the right flange
- The blue curve corresponds with the stress in the web
- The green curve corresponds with the stress in the left flange.

The first critical stress is 177.5 N/mm^2. This value is half of the yield stress (the residual stress is the other half). The stress in the left flange (for the column length of twelve meters) does not reach the first critical stress. The column fails if the whole right flange yields. This occurs at a stress of 532.5 N/mm^2 (1.5 times the yield stress). The stress in the left flange of the column of ten meters reaches the first critical stress. According to the chosen residual stress distribution (Fig. 5.7), the half of the left flange yields. Due to this yielding, the effective cross-section decreases. The stress in the effective cross-section increases. A lower ultimate load can be found. The same situation had been found in the analysis of the single column (see the blue curve of Fig. 5.12).

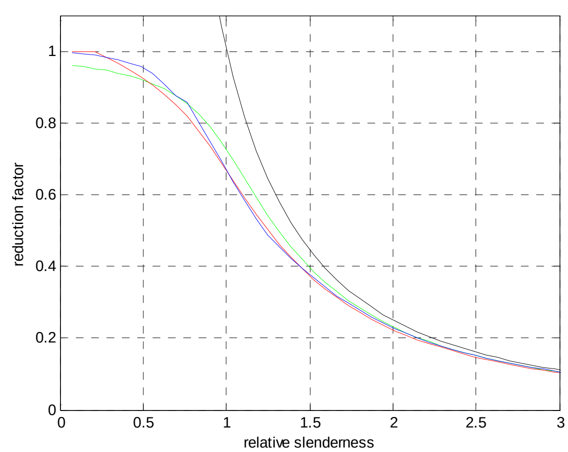

Figure 5.12: Stability curve for several calculations methods

The second striking point is the large difference between the calculation according to the Dutch code and the calculation according to the other calculation methods. The explanation of this is the safety in the Dutch code. The beam is very stiff compared with the column. This results in almost fixed ends of the column. This very stiff connection is used in the ultimate load calculation of the analysis and in the Matrix Frame calculations. According to the ultimate load calculation according to the Dutch code, it is not possible to create such a connection. The connections are taken less stiff. This results in a larger buckling length. For slender structures, the buckling length is an important factor of the ultimate load calculation. Due to this increase of the buckling length, the ultimate loads deceases.

With the exception of the ultimate load of the non-slender structures, the results of the analysis correspond with the results of the Matrix Frame calculations. The residual stress of the Matrix Frame calculation is less than the residual stress in the analysis. This cannot be solved because of input limitations of Matrix Frame. The analysis results in proper ultimate loads and can be used.

Chapter 6 Conclusions and recommendations

The buckling loads of four steel frame structures have been derived analytically and numerically. The analyses included physical modelling of shape deviations and residual stresses. The results have been compared to those of code equations. These code equations also include the effect of shape deviations and residual stresses due to an extensive experimental program.

Conclusions

Due to residual stresses, a frame structure partially yields before it fails. If the structure partial yields, the effective cross-section and the effective stiffness decrease. A decreased section changes the course of the deflection. For every yielding part another formula must be derived. A realistic residual stress distribution is smooth and results in infinite numbers of formulas. The applied residual stress distribution has three yield levels. The analyses result in three formulas of the additional deflection.

An analytical non-linear analysis of a steel frame structure is very time consuming. However, the resulting formulas are very attractive. Computer programs like Excel and MatLab can be used to calculate the ultimate load. Using variable parameters, the section properties and the length of the sections can be changed easily. This is very helpful in a design situation.

Without imperfections the ultimate load predicted with non-linear finite element computer programs (such as Matrix Frame) are considerably larger than the ultimate load according to the Dutch code. With shape derivations and residual stresses will be introduced, the results of the Matrix Frame calculation are close to the results of the code rules.

Matrix Frame cannot calculate with curved sections. The initial geometrical imperfections can only be introduced by splitting the column in small parts. All these parts are fixed together and every joint has a different location. Using initial geometrical imperfections influence the deflections that are computed in a geometrical non-linear analysis.

Residual stresses result in partial yielding of a section. To take residual stresses into account a section can be modelled by two elements (with different yield stresses and half the original cross-section properties). However, Matrix Frame does not properly calculate sections with different yield properties. It does not distribute the load properly over the two elements. A consequence of this is that an overall analysis is not possible. As a solution the geometrical and physical non-linear analyses can be performed for each cross section half. The summation of these analyses is approximately the ultimate load.

Special attention is needed for the calculations of very non-slender columns with fixed ends. Due to the partial yielding (as a result of the residual stresses) the column can deflect easier and the bending moment at the end of the column decreases. This results in a larger ultimate load.

Recommendations

As yet it was not possible to find a general buckling formula for all structures. For a general formula more analyses must be made. Also all analyses need to have the same boundary conditions. Using proper boundary conditions, it could be possible to find a general formula in further analyses. This is an interesting object for another master thesis.

Matrix Frame has an input limitation. It is not possible to choose the yield stress freely. Only the usually steel grades can be chosen. Because of this, it is not possible to take care of all residual stresses for all steel grades. For small HEA sections the amount of residual stress is larger than for large HEA sections. The amount of residual stress for small HEA sections cannot be inserted. Steel grade S355 is the only steel grade that can be used for the calculations including residual stresses. For checking the analysis results, it would be better to make a possibility to insert the yield stress manually.

The differences in ultimate loads between different calculation methods are largest for non-slender structures. Matrix Frame 'solved' this problem by using a smaller yield stress. It is recommended to check the ultimate loads for frames with non-slender columns.

Matrix Frame is commonly used in current practice and is specialized in Frame type structures. Because of this Matrix Frame is used in this study. Unfortunately, residual stresses and also reduced stiffness cannot be modelled in Matrix Frame. Other (more complex) computer programs without these limitations could give in better results. Because of time limitation no other computer programs has been used.

Bibliography

[1] Verburg, W.H., Overspannend staal deel 1 Basisboek, Rotterdam, 2004
[2] Man de, D., Overspannend staal deel 2 Construeren A, Rotterdam, 2001
[3] Rolloos, A. and Spil, B.C.A., Overspannend staal deel 3 Construeren B, Rotterdam, 1996
[4] Broek van den, T.J., Overspannend staal deel 5 Staalprofielen, Rotterdam, 1998
[5] Hartsuijker, C., Toegepaste mechanica deel 1 evenwicht, Nootdorp, 2005
[6] Hartsuijker, C., Toegepaste mechanica deel 2 spanningen, vervormingen, verplaatsingen, Nootdorp, 2005
[7] Hartsuijker, C., Toegepaste mechanica deel 3 statisch bepaalde constructies en bezwijkanalyse, Nootdorp, 2005
[8] Vrouwenvelder, A.C.W.M., Lecture notes CT5144 Structural Stability, Delft, 2003
[9] Vrouwenvelder, A.C.W.M., Lecture notes CT4150 Plastic Analysis of Structures, Delft, 2003
[10] Simone, A., Lecture notes CT3110 Analysis of slender structures, Delft, 2007
[11] Gresnigt, A.M., Lecture notes CT3121 Steel structures II, Delft 2004
[12] Grit, R., Projectmanagement, Groningen, 2000
[13] Boer de, H. and Bood de, E.G., Wolters ster woordenboek Nederlands - Engels, Groningen, 1996
[14] Boer de, H. and Bood de, E.G., Wolters ster woordenboek Engels - Nederlands, Groningen, 1996
[15] Nederlands Normalisatie – instituut, NEN 6770 staalconstructies – basiseisen en rekenregels, 1997
[16] Nederlands Normalisatie – instituut, NEN 6771 staalconstructies – stabiliteit, 2000
[17] Nederlands Normalisatie – instituut, NEN 6702 belastingen en vervormingen, 2001
[18] Boon, J., Restspanningen in stalen UNP 160 profielen, 2001
[19] Several internet sides. The following sites are the most used sites:

- http://www.mechanics.citg.tudelft.nl
- http://www.scopus.com
- http://woordenboek.tudelft.nl
- http://www.library.tudelft.nl
- http://babelfish.yahoo.com